Differential deregulation of NGF and BDNF neurotrophins in a transgenic rat model of Alzheimer's disease

M. Florencia Iulita[a,1], M. Beatriz Bistué Millón[b,1], Rowan Pentz[c], Lisi Flores Aguilar[d], Sonia Do Carmo[a], Simon Allard[a], Bernadeta Michalski[e], Edward N. Wilson[c], Adriana Ducatenzeiler[a], Martin A. Bruno[b], Margaret Fahnestock[e], A. Claudio Cuello[a,c,d,*]

[a] Department of Pharmacology and Therapeutics, McGill University, Montreal, Canada
[b] Facultad de Ciencias Médicas, Universidad Católica de Cuyo-CONICET, San Juan, Argentina
[c] Department of Neurology and Neurosurgery, McGill University, Montreal, Canada
[d] Department of Anatomy and Cell Biology, McGill University, Montreal, Canada
[e] Department of Psychiatry and Behavioural Neurosciences, McMaster University, Hamilton, Canada

ABSTRACT

Evidence from human neuropathological studies indicates that the levels of the neurotrophins nerve growth factor (NGF) and brain-derived neurotrophic factor (BDNF) are compromised in Alzheimer's disease. However, the causes and temporal (pathology-dependent) evolution of these alterations are not completely understood. To elucidate these issues, we investigated the McGill-R-Thy1-APP transgenic rat, which exhibits progressive intracellular and extracellular amyloid-beta (Aβ) pathology and ensuing cognitive deficits. Neurochemical analyses revealed a differential dysregulation of NGF and BDNF transcripts and protein expression. While BDNF mRNA levels were significantly reduced at very early stages of amyloid pathology, before plaques appeared, there were no changes in NGF mRNA expression even at advanced stages. Paradoxically, the protein levels of the NGF precursor were increased. These changes in neurotrophin expression are identical to those seen during the progression of Alzheimer's disease. At advanced pathological stages, deficits in the protease cascade controlling the maturation and degradation of NGF were evident in McGill transgenic rats, in line with the paradoxical upregulation of proNGF, as seen in Alzheimer's disease, in the absence of changes in NGF mRNA. The compromise in NGF metabolism and BDNF levels was accompanied by downregulation of cortical cholinergic synapses; strengthening the evidence that neurotrophin dysregulation affects cholinergic synapses and synaptic plasticity. Our findings suggest a differential temporal deregulation of NGF and BDNF neurotrophins, whereby deficits in BDNF mRNA appear at early stages of intraneuronal Aβ pathology, before alterations in NGF metabolism and cholinergic synapse loss manifest.

1. Introduction

Alzheimer's disease is the leading cause of dementia in the elderly. Its hallmark brain lesions include extracellular amyloid plaques primarily composed of aggregated amyloid-beta (Aβ) peptides and intracellular neurofibrillary tangles composed of abnormally phosphorylated tau filaments (Goedert et al., 1988; Grundke-Iqbal et al., 1986; Terry, 1997). It is increasingly recognized that soluble oligomeric forms of Aβ are more toxic and contribute more to neurodegeneration than the classical insoluble plaques (Cleary et al., 2005; Jin et al., 2011; Lambert et al., 1998; Lesne et al., 2006; Shankar et al., 2008; Walsh et al., 2002). Furthermore, several studies suggest that

intraneuronal Aβ, even in the absence of plaques, has toxic effects on central nervous system (CNS) functions (Billings et al., 2005; Echeverria et al., 2004; Ferretti et al., 2012; Iulita et al., 2014a; Oddo et al., 2003; Wilson et al., 2016).

Additional factors that contribute to cognitive dysfunction in Alzheimer's disease include synaptic and neuronal loss (DeKosky and Scheff, 1990; Selkoe, 2002), neuroinflammation (Eikelenboom et al., 1998; McGeer et al., 1987; Parachikova et al., 2007) and basal forebrain cholinergic neurodegeneration (Bowen et al., 1976; Davies and Maloney, 1976; Etienne et al., 1986; Mufson et al., 1989; Mufson et al., 2000; Pearson et al., 1983; Vogels et al., 1990; Whitehouse et al., 1982). Basal forebrain cholinergic neurons are the main source of acetylcholine to the cortex and hippocampus (Mesulam et al., 1983). These neurons are highly vulnerable to Alzheimer's pathology. They are some of the earliest to degenerate and become atrophic (Pearson et al., 1983; Schmitz et al., 2016; Whitehouse et al., 1982). Given the key role of cholinergic input to higher CNS functions such as learning, memory (Bartus et al., 1982; Drachman and Leavitt, 1974) and attention (Sarter et al., 2003), the progressive loss of cognitive function characteristic of Alzheimer's disease has been attributed in part to the degeneration of this transmitter system (Coyle et al., 1983).

Basal forebrain cholinergic neurons have a life-long dependence on the retrograde supply of the neurotrophin nerve growth factor (NGF) for the maintenance of their cholinergic phenotype, even in the adult and fully differentiated brain (Cuello, 1996). Neurotrophins are a family of proteins including NGF, BDNF, NT-3 (neurotrophin 3) and NT-4/5 (neurotrophin 4/5), which have crucial roles in the survival, growth and differentiation of neurons during development (Allen and Dawbarn, 2006; Bibel and Barde, 2000) and whose trophic signals are equally vital in the adult brain for neuronal phenotypic maintenance (Cuello, 1996; Thoenen, 1995).

BDNF is an important regulator of learning and memory processes. Mature BDNF strengthens synapses, whereas proBDNF weakens synapses, making the ratio of proBDNF to BDNF important for synaptic plasticity (Je et al., 2012; Yang et al., 2014). BDNF also upregulates ChAT activity (the enzyme responsible for the synthesis of acetylcholine) and promotes the survival of septal developing neurons (Klein et al., 1999; Knusel et al., 1991; Nonomura and Hatanaka, 1992). BDNF mRNA, its precursor (proBDNF) and mature protein levels are decreased by half in entorhinal, frontal, temporal and parietal cortex, hippocampus and basal forebrain of Alzheimer's disease brains (Connor et al., 1997; Ferrer et al., 1999; Garzon et al., 2002; Hock et al., 2000; Holsinger et al., 2000; Michalski and Fahnestock, 2003; Peng et al., 2005; Phillips et al., 1991) and in several mouse models of amyloid pathology (Francis et al., 2012; Peng et al., 2009). These are areas of the brain that are associated with learning and memory and are severely affected in Alzheimer's disease (Burns and Illiffe, 2009). The reduction in BDNF expression occurs early in disease progression, prior to plaque deposition in transgenic animals (Francis et al., 2012), and correlates with the degree of cognitive deficits in humans (Buchman et al., 2016; Peng et al., 2005).

Paradoxically, no changes in the levels of NGF mRNA in the cerebral cortex of subjects with Alzheimer's disease have been observed (Fahnestock et al., 1996; Goedert et al., 1986; Jette et al., 1994), while the levels of the NGF precursor molecule, proNGF, are increased (Bruno et al., 2009a; Fahnestock et al., 2001; Pedraza et al., 2005; Peng et al., 2004). *Ex-vivo* pharmacological studies in normal rats further demonstrated that endogenous NGF is released as a precursor (proNGF) in an activity-dependent manner, along with the enzymes, zymogens and regulators necessary for its proteolytic processing to mature NGF and its subsequent degradation outside the cell (Bruno and Cuello, 2006). In this pathway, referred to as *the NGF metabolic cascade*, proNGF is converted to mature NGF by plasmin, a serine protease that derives from plasminogen when cleaved by tissue plasminogen activator (tPA). In the CNS, tPA activity is inhibited by neuroserpin (Miranda and Lomas, 2006). The extracellular enzymatic degradation of mature NGF is accomplished by matrix metallo-protease 9 (MMP-9) (Bruno and Cuello, 2006), whose activity is attenuated by tissue inhibitor of metallo-proteases 1 (TIMP-1) (Rosenberg, 2009). Thus, the discovery of the NGF metabolic cascade provided a new platform by which to re-examine the causes of proNGF accumulation and the compromised cholinergic trophic supply observed in CNS β-amyloid pathologies [for reviews see: (Cuello and Bruno, 2007; Iulita and Cuello, 2014; Iulita and Cuello, 2016)].

Studies examining cortical homogenates from Alzheimer patients, and from individuals with Down syndrome with Alzheimer's dementia, revealed a reduction in the levels of plasminogen and tPA; suggesting that these changes should impair the maturation of proNGF and explain its paradoxical accumulation in Alzheimer's disease (Bruno et al., 2009a; Iulita et al., 2014b). Upregulation of MMP-9 activity, the main NGF-degrading protease, was also evident, suggesting greater NGF degradation (Bruno et al., 2009a; Iulita et al., 2014b). Taken together, these alterations suggest that the availability of NGF to forebrain cholinergic neurons is affected in Alzheimer's disease, a scenario that is consistent with the presence of severe cholinergic deficits.

NGF and BDNF dysregulation are evident even in mild cognitive impairment (MCI) (Bruno et al., 2009b; Peng et al., 2004; Peng et al., 2005), considered a prodromal stage of Alzheimer's disease. However, considering that Alzheimer's pathology develops decades before dementia onset (Dubois et al., 2016), it is important to determine how early during disease progression these alterations in NGF and BDNF appear. This question remains difficult to answer in humans given the lack of suitable biomarkers that can reliably detect Alzheimer's dementia during its silent (asymptomatic) stages. In that sense, transgenic models of AD-like amyloid pathology can offer an advantage given that these animals progressively accumulate intraneuronal Aβ peptide, exhibit amyloid plaques and develop cognitive deficits. Thus, the goal of this study was to investigate the evolution of NGF and BDNF deregulation and the impact on cholinergic synapses during the progression of Aβ pathology in an advanced animal model of Alzheimer's disease, the McGill-R-Thy1-APP transgenic rat. Compared to mice, rats are physiologically, genetically, and morphologically closer to humans, offering a more accurate representation of the human disease to answer this question (Do Carmo and Cuello, 2013).

2. Materials and methods

2.1. Transgenic rats

All procedures were approved by the Animal Care Committee of McGill University, and conformed with the ARRIVE guidelines and with those of the Canadian Council on Animal Care. Homozygous and hemizygous transgenic rats (APP +/+ and APP +/−, respectively) belonged to the McGill-R-Thy1-APP line, overexpressing human APP751 incorporating the Swedish and Indiana mutations under the control of the Thy1.2 promoter (Leon et al., 2010). Genotyping was done by qPCR using human APP-specific primers (Forward: ATCCCA-CTCGCACAGCAG; Reverse: GGAATCACAAAGTGGGGATG).

Animals belonged to one of three groups: young (3–6 months old), middle-aged (13–15 months) and old (18–21 months). Age-matched wild type rats, used as controls, were non-transgenic littermates (hAPP negative, APP −/−). Animals were maintained on a 12-hour light dark/cycle and had *ad libitum* access to water and a standard rodent diet. Male and female rats were used for this study in approximately equal numbers. A minimum of $n = 5$–6 rats per genotype per time point were used for all experiments. The precise number of animals used per experiment is specified in Results and in the figure legends.

2.2. Brain tissue collection

Rats were anesthetized with equithesin (6.5 mg of chloral hydrate and 3 mg of sodium pentobarbital in a volume of 0.3 ml, i.p., per 100 g

of body weight) and perfused transcardially with cold 0.2 M phosphate buffer for 1–2 min. The brain was removed; one cortical hemisphere was dissected, flash-frozen, and kept at − 80 °C for qRT-PCR, Western blot and zymography analysis. The other hemisphere was kept intact for immunohistochemistry. In parallel to human studies on BDNF and NGF levels in Alzheimer brains, the cortex was used for analysis.

2.3. Immunohistochemistry

Hemi-brains were immersed in cold 4% paraformaldehyde (Fisher Scientific, USA) in 0.1 M phosphate buffer for 24 h and then transferred to 30% sucrose (dissolved in 0.1 M phosphate buffer). Brains were stored in cryoprotectant solution [37.5% v/v ethylene glycol, 37.5% w/w sucrose, in phosphate-buffered saline (PBS) pH 7.4] at − 20 °C until further use. Free-floating immunostaining was done according to established protocols (Côté et al., 1994; Ferretti et al., 2011; Hu et al., 2003; Iulita et al., 2014a; Leon et al., 2010). Brains were cut into 40 μm coronal sections with a freezing microtome (Leica SM 2000R, Germany). For all immunolabelings, omission of primary antibodies was done to confirm signal specificity.

2.3.1. Analysis of amyloid pathology

Rat brain sections were incubated in 0.3% hydrogen peroxide for 20 min, washed three times in PBS-T (0.2 M phosphate-buffered saline, 0.2% Triton X-100) and blocked 1 h with 10% goat serum (Millipore, USA) in PBS-T. Aβ pathology was examined with a monoclonal antibody specific for the human Aβ peptide (McSA1, MediMabs, Montreal, Canada) (Table 1) (Grant et al., 2000); applied at 1:4000 in PBS-T with 5% goat serum, overnight at 4 °C. The following day, sections were incubated in goat anti-mouse secondary antibody (MP Biochemicals, Canada) at 1:100 in PBS with 5% goat serum for 1 h at room temperature, following by a 1 h incubation with a mouse anti-peroxidase monoclonal antibody (Semenenko et al., 1985) at 1:30, pre-incubated with horseradish peroxidase (5 μg/ml) (MAP kit, Medimabs, Canada). Immunohistochemical stainings were developed with 0.06% 3,3′-diaminobenzidine (DAB) (Sigma-Aldrich, USA) and 0.01% hydrogen peroxide (Sigma-Aldrich, USA) in PBS and mounted on subbed slides. Prior to coverslipping (Entellan, EM Science, USA), sections were dehydrated and defatted in increasing ethanol concentrations (70–100%) and xylene for 15 min (each step). Bright-field images were acquired on an Axioplan microscope equipped with an AxioCam HRc digital camera (Carl Zeiss, Toronto, Canada) with Axiovision 4.8 Software.

2.3.2. Analysis of cholinergic varicosities

For immunohistochemical detection of vesicular acetylcholine transporter (VAChT)-immunoreactive cholinergic boutons, rat brain sections were washed with PBS and incubated in 0.3% hydrogen peroxide in PBS for 20 min to quench endogenous peroxidase. Sections were then washed in PBS-T and incubated overnight in 10% normal goat serum (NGS)-PBS-T at 4 °C. The following day, brain sections were incubated with a rabbit anti-VAChT primary antibody (Synaptic Systems, Germany) (Table 1) at 1:1000, overnight at 4 °C. After this step, rat brain sections were washed three times in PBS and then incubated with a biotinylated goat anti-rabbit antibody (1:200, Vector Laboratories, USA) overnight at 4 °C. Following incubation with the secondary antibody, the sections were washed with PBS and incubated in ABC Vectastain Elite kit (Vector Laboratories, USA), for 1 h (1:250 A + 1:250 B in PBS, prepared 30 min before incubation). The sections were washed and then incubated in 0.05% 3,3′-diaminobenzidine (DAB) for 10 min. The reaction was developed by adding hydrogen peroxide (1:3000) and stopped after 7 min by washing in PBS. The sections were mounted on gelatin-subbed slides, dehydrated and defatted using ascending alcohols then xylenes, and coverslipped (Entellan, EM Science, USA).

Bright field images were captured using a Zeiss Axio Imager M2 microscope equipped with a Zeiss Axiocam 506 color digital camera

Table 1
List of primary antibodies used for immunohistochemistry and Western blotting.

Antibody target	Specificity	Antibody and source	Epitope	Dilutions	Source/company
McSA1	Human, mouse	Mouse monoclonal to human Aβ	Residues of 1–12 of human Aβ	1/4000	MediMabs, Montreal Canada
6E10	Human	Mouse monoclonal to human Aβ	Residues of 1–16 of human Aβ	1/1000	Covance, USA
proNGF	Human	Rabbit polyclonal to proNGF	Pro-domain of rat NGF (84–104 aa)	1/1000	Alomone Labs, Israel
BDNF	Human, mouse, rat	Rabbit polyclonal to BDNF	Internal region of BDNF of human origin	1/500	Santa Cruz Biotechnology, USA
tPA	Human	Goat polyclonal to tPA	Human tPA	1/500	American Diagnostica, USA
Neuroserpin	Rat	Rabbit polyclonal to neuroserpin	Human neuroserpin	1/10000	Dr D. Lawrence, University of Michigan
Plasminogen	Human, mouse, rat	Rabbit polyclonal to plasminogen	N-terminus of human plasminogen	1/1000	Santa Cruz Biotechnology, USA
MMP-9	Human, mouse, rat, dog	Rabbit polyclonal to MMP-9	Full-length MMP-9 native protein	1/1000	Abcam, USA
TIMP-1	Human, mouse, rat	Rabbit polyclonal to TIMP-1	C-terminus (aa 58–207) of human TIMP-1	1/500	Santa Cruz Biotechnology, USA
β III-tubulin	Human and rat	Mouse monoclonal to β III-tubulin	C-terminus (peptide, EAQGPK) of β III-tubulin	1/50000	Promega, USA
α-Tubulin	Yeast, human, chicken, rat, amphibian, fungi, bovine, mouse	Mouse monoclonal to α-tubulin	C-terminus of α-tubulin	1/4000	Sigma, USA
β-Actin	Guinea pig, mouse, chicken, sheep, rabbit, rat, human, bovine	Mouse monoclonal to β-actin	N-terminus of β-actin	1/4000	Sigma, USA
GAPDH	Human, mouse, rat, canine, feline, porcine, rabbit	Mouse monoclonal to GAPDH	Mouse, rat, human GAPDH	1/5000	Millipore, USA
VAChT	Human, rat, mouse, hamster	Rabbit polyclonal to VAChT (#139103)	C-terminal part of rat VAChT (aa 475–530)	1:1000	Synaptic Systems, Germany

coupled to Zeiss ZEN 2 (blue edition) software. In order to quantify cholinergic bouton density, digital images from lamina V of the parietal cortex and CA2-CA3 regions of the hippocampus were acquired. Five images were captured per cortical section and four images per hippocampal section, for a total of five sections per animal. Images were analyzed using ImageJ (National Institutes of Health, USA). Immunoreactive material was separated from background using optical density and size criteria. More precisely, the optical intensity threshold was established using the 'triangle' algorithm (Zack et al., 1977). Following thresholding, immunoreactive structures of a size ranging from 0.2 μm^2 to 6 μm^2 were included in the varicosity count. The varicosity counts are expressed as a density of boutons in an imaging field of 30,000 μm^2.

2.4. RNA extraction and quantitative reverse transcription-polymerase chain reaction

For all transcript analysis except for BDNF (see description below), quantitative real-time RT-PCR (qRT-PCR) was carried out as previously detailed (Iulita et al., 2014b; Taylor et al., 2010). Cortex samples were homogenized using the QIAshredder (Qiagen, USA) and total RNA was purified using an RNA Isolation kit (Qiagen, USA) according to the manufacturer's protocol. The ratio of absorbance at 260 nm to 280 nm was used to confirm the purity of RNA samples using the NanoDrop spectrophotometer (BioRad, USA). cDNA was synthesized using the BioRad iSCRIPT kit (#1725122, BioRad, USA) in a 20-μl reaction containing 250–500 ng of total RNA. For all qRT-PCR reactions, 10 μM of the forward and reverse primers were used (Table 2). Real-time PCR was performed in a 10-μl reaction containing 2 μl of cDNA with iQ SYBR® Green (BioRad, USA) in a Bio-Rad iCycler. PCR was performed by initial denaturation at 95 °C for 15 min, followed by 40 cycles of 10 s at 95 °C, 30 s at 60 °C, and 15 s at 72 °C. Real time amplification was completed in triplicate. Specificity was verified by melting curve analysis and *via* agarose gel electrophoresis. The threshold cycle (Ct) values of each sample were used in the post PCR data analysis. Cortical mRNA expression was quantified relative to non-transgenic rats using the DDCt (delta delta Ct) method, with HPRT (hypoxanthine-guanine phosphoribosyltransferase) as the housekeeping gene. Standard curve R2 values were > 0.99 and efficiencies were between 90% and 110% for all primers used.

For BDNF analysis, RNA extraction and qRT-PCR were carried out as previously described (Michalski et al., 2015; Willand et al., 2016). RNA was extracted from frozen rat cortical tissue in TRIzol® (Invitrogen, Canada) at a ratio of 1 ml of TRIzol® per 50 mg of tissue using a sonic dismembrator (Fisher Scientific, Canada). Invitrogen's protocol was followed through the collection of the RNA-containing aqueous phase. The RNA was further purified and DNase-treated using an RNeasy® Mini Kit (Qiagen, Canada) according to the manufacturer's instructions. Concentration and purity of RNA were confirmed by absorbance at 260, 280 and 230 nm using a Thermo Scientific NanoDrop 2000c (Fisher Scientific, Canada). One microgram of each RNA sample was reverse transcribed in a 20 μl reaction using Superscript III® (Invitrogen,

Canada) following the manufacturer's protocol. Negative controls lacking reverse transcriptase were included to confirm absence of genomic DNA contamination.

For all PCR reactions, 300 nM of rat BDNF or β-actin primers (Table 2) were used. Each 20 μl real-time PCR reaction contained 10 μl of SYBR® Green qPCR SuperMix (Invitrogen, Canada), 30 nM of reference dye ROX (Invitrogen, Canada) and cDNA derived from 50 ng RNA per sample or standards. Standards for BDNF and β–actin were PCR products generated using target-specific primers. PCR products were gel purified using a Qiagen kit and quantified by spectrophotometry (Thermo Scientific NanoDrop 2000c). Real-time amplifications were carried out in triplicate using the MX3000P PCR system (Stratagene, USA) and the following thermal profile: 2 min at 50 °C, 2 min at 95 °C followed by 40 cycles of 95 °C for 30 s, 58 °C for 30 s, and 72 °C for 45 s for BDNF. Standard curve R2 values were > 0.995 and efficiencies were > 90%. Following 40 cycles of amplification, a dissociation curve was added to determine if any secondary products had formed. Absolute numbers of mRNA copies were determined with respect to the standard curve. Cortical mRNA copy numbers of BDNF are presented as a ratio to copy numbers of β-actin, and expressed relative to that of non-transgenic rats.

2.5. Western blotting

For all proteins except for BDNF (see description below), frozen rat cortex samples were manually homogenized in 8 × w/v cold lysis buffer (50 mM Tris HCl pH 7.4; 150 mM NaCl; 1% Nonidet P-40; 0.1% SDS) containing protease inhibitors (Roche, USA). Manual homogenization was followed by three 5 s pulses of sonication. Cortical homogenates were centrifuged at 13.000 rpm, 45 min at 4 °C and the supernatants were kept at − 80 °C until further analysis. Protein concentration was measured with the DC™ Protein Assay kit (BioRad, USA). Protein from cortical homogenates (30–50 μg) were separated on 8–12% SDS-polyacrylamide gels under reducing conditions and transferred semi-dry to nitrocellulose membranes (BioRad, USA) for 1 h at 300 mA. Membranes were blocked in 5% skim milk or bovine serum albumin (BSA, Sigma, USA) for 1 h at room temperature and incubated with primary antibodies in blocking solution overnight at 4 °C. A detailed description of the antibodies used is depicted in Table 1. Peroxidase-conjugated secondary antibodies (Jackson Immunoresearch, USA), dissolved in blocking solution, were applied for 1 h at room temperature (dilution 1:10,000). Recombinant tPA (American Diagnostica, USA) and a whole cell lysate from B cell lymphoma cells overexpressing plasminogen (Santa Cruz Biotechnology, USA) were used as positive controls.

For detection of APP and its metabolic products with the 6E10 anti-human Aβ monoclonal antibody (Covance, USA), 120 μg proteins from rat cortical homogenates were separated on 10–20% Tris-tricine gels (Criterion, BioRad, USA) under reducing conditions. Prior to electrophoresis, samples were boiled for 15 s in sample loading buffer (BioRad, USA). Proteins were transferred semi-dry to nitrocellulose membranes (BioRad, USA) for 2 h at 220 mA. Following transfer, membranes were

Table 2
List of primers used.

Gene	Species	Forward 5′3′	Reverse 5′3′	Size (bp)
NGF	*Rattus norvegicus*	CAACAGGACTCACAGGAGCA	GTCCGTGGCTGTGGTCTTAT	115
BDNF	*Rattus norvegicus*	GCGGCAGATAAAAAGACTGC	GCAGCCTTCCTTCGTGTAAC	141
tPA	*Rattus norvegicus*	GTGAAGCCCTGGTGCTATGT	GCCACGGTAAGTCACACCTT	123
Plasminogen	*Rattus norvegicus*	GGTGGGAGGCAGAACAAAAC	GGGTGACAGGAAGTAGTGGT	114
Neuroserpin	*Rattus norvegicus*	ATGAGGCTGGTGGCATCTAC	GATCAGCTGTGGTTTGAGCA	131
MMP-9	*Rattus norvegicus*	CCAGCATCTGTATGGTCGTG	GAGGTGCAGTGGGACACATA	107
TIMP-1	*Rattus norvegicus*	GAACGGAAATTTGCACATCA	ATGGCTGAACAGGGAAACAC	135
Furin	*Rattus norvegicus*	GCCTTCTTTCGGGGAGTTAG	GCTGATGGACAGCGTGTAGA	138
β-Actin	*Rattus norvegicus*	AGCCATGTACGTAGCCATCC	CTCTCAGCTGTGGTGGTGAA	228

incubated in boiling PBS for 5 min and were subsequently blocked with 7.5% milk for 2 h. Following the blocking step, membranes were incubated with the primary antibody (6E10) at a concentration of 1:1000, overnight at 4 °C. Peroxidase-conjugated anti-mouse secondary antibody (Jackson Immunoresearch, USA), dissolved in blocking solution, was applied for 1 h at room temperature (dilution 1:5000).

Western blots were developed with an enhanced chemiluminescence substrate (Western Lightning® Plus-ECL, PerkinElmer Inc., USA). Densitometry (IOD) was quantified with TotalLab CLIQS Software (TotalLab, UK) and/or Gel-Pro analyzer Software (Media Cybernetics, Inc.). Densitometry values (IOD) were normalized to the loading control (βIII-tubulin or GAPDH) and expressed as fold change relative to the control group.

For BDNF protein analysis, frozen rat cortical tissue was sonicated in RIPA buffer containing 50 mM Tris pH 7.5, 150 mM NaCl, 10 mM EDTA, 0.1% SDS, 1% Nonidet P-40, 0.1% sodium deoxycholate and protease and phosphatase inhibitor cocktails (Roche, Canada) using a sonic dismembrator (Fisher Scientific, Canada) at a ratio of 1.5 ml of buffer per 100 mg of tissue. The homogenates were kept on ice for 10–15 min and then centrifuged at $14000 \times g$ for 20 min at 4 °C. Supernatants were collected, aliquoted, and kept frozen at − 80 °C until use. Protein concentration was established using the DC™ protein assay (BioRad, Canada). A total of 50 μg of each cortical homogenate was resolved on a 12% polyacrylamide gel or a TGX precast gradient gel (BioRad, Canada). Gel electrophoresis and transfer were carried out as previously described (Michalski and Fahnestock, 2003) with the exception that Immobilon-FL membranes were used (Millipore, Canada). Membranes were incubated for 48–72 h with rabbit polyclonal BDNF N-20 antibody at 4 °C (Santa Cruz, USA). Blots were also probed overnight with α-tubulin or β-actin antibody (Sigma, Canada). Primary and secondary antibodies (Goat Anti-rabbit IRDye® 680 and Goat Anti-Mouse IRDye® 800CW; LI-COR® Biosciences, USA; dilutions 1:8000) were diluted in Odyssey Blocking Buffer (LI-COR®, Biosciences, USA) mixed 1:1 with PBS and containing 0.05% Tween-20. Signals were detected and quantified using an Odyssey Imaging System (LI-COR®, Biosciences, USA). Densitometry values for BDNF and proBDNF were normalized to the loading control (α-tubulin or β-actin) and expressed as fold change relative to the control group. Relative values of total BDNF protein were validated with the Human BDNF DuoSet ELISA kit (R & D Systems, USA), which, in our hands, has a detection range of 6–1500 pg/ml. Each sample was adjusted to a concentration of 1 mg/ml, and both standards and samples were assayed in duplicate following the manufacturer's protocols. Values obtained by ELISA were expressed as pg of BDNF per mg of total protein.

2.6. MMP-9 gelatin zymography

The proteolytic activity of MMP-9 (~ 92 kDa) and MMP-2 (~ 72 kDa) was determined by gelatin zymography, as previously described (Bruno et al., 2009a; Bruno et al., 2009b; Iulita et al., 2014b). Briefly, 70 μg of rat cortical homogenates were separated on 8% SDS-polyacrylamide gels containing 0.2% gelatin (Sigma-Aldrich, USA). Electrophoresis was run on ice. Following two rinses with water, zymograms were incubated in renaturing solution (2.5% Triton X-100; Sigma-Aldrich, USA) for 45 min at room temperature. Digestion was carried out at 37 °C in developing buffer (50 mM Tris, 0.2 M NaCl, 5 mM CaCl$_2$, Brij-35 0.02%) for 45 h. Zymograms were stained for 1 h in 0.25% Coomasie R-250 (BioRad, USA) and destained with a solution of methanol, water, and acetic acid (50:40:10), until clear areas of gelatinase activity were seen against the dark-stained background. Gels were imaged and digitized (AlphaDigidoc System, USA) for quantification with TotalLab CLIQS Software (TotalLab, UK).

2.7. Statistical analysis

The software GraphPad Prism v5.01 (La Jolla, CA, USA) was used

for statistical analysis. Data normality was verified with the D'Agostino and Pearson omnibus K2 normality test. A two-tailed Student's *t*-test was used for 2-group comparisons. A one-way ANOVA was used for three-group comparisons, followed by post-hoc multiple comparison tests (Bonferroni correction). Pearson correlation analysis was used to investigate associations between BDNF mRNA and cognitive deficits. The latter were expressed as a cognitive composite (Z_global) of the rats' performance in the novel object recognition and location tasks as well as in fear conditioning. This parameter and the resulting data have been calculated and published elsewhere (Iulita et al., 2014a). Significance was set at $p < 0.05$. Graphs illustrate mean ± SEM.

3. Results

3.1. Evolution of amyloid pathology in McGill-R-Thy1-APP transgenic rats

A detailed description of the time-dependent progression of Alzheimer-like amyloid pathology in McGill-R-Thy1-APP rats has been previously reported (Hanzel et al., 2014; Iulita et al., 2014a; Leon et al., 2010; Wilson et al., 2016). In this transgenic rat, a single APP transgene leads to the intracellular accumulation of Aβ in pyramidal neurons of the cerebral cortex and hippocampus. Aβ accumulation progresses with age, being detectable as early as 1 week, and is strongly established in 3–6 month-old rats (Fig. 1A). This early stage (3–6 months) is characterized by significant cognitive impairments (Galeano et al., 2014; Iulita et al., 2014a; Leon et al., 2010; Pimentel et al., 2015; Wilson et al., 2016) and by deficits in *in vivo* LTP (Qi et al., 2014). At these time points, there is robust expression of soluble Aβ42 in cortex as well as intracellular Aβ oligomers (Iulita et al., 2014a) and a strong pro-inflammatory process (Hanzel et al., 2014).

As the pathology advances, isolated extracellular Aβ deposits (amyloid plaques) may occasionally appear in homozygous transgenic rats starting at 6 months of age (Leon et al., 2010), whereas progressive amyloid deposition occurs from 8 to 9 months onwards (Iulita et al., 2014a; Pimentel et al., 2015; Wilson et al., 2016). By 13–15 months, both diffuse and dense (fibrillar) plaques can be detected in most areas of the hippocampal formation and to a lesser extent in the cerebral cortex (Fig. 1B).

Finally, in 18–21 month-old homozygous rats, amyloid plaques can be found in most areas of the cerebral cortex, particularly in the hippocampus, as well as in the entorhinal and parietal cortices (Fig. 1C). These plaques have been previously described as being of fibrillary nature as assessed with Thioflavin S staining (Leon et al., 2010). Cognitive deficits further advance at the post-plaque stage (Galeano et al., 2014; Iulita et al., 2014a; Leon et al., 2010; Pimentel et al., 2015), and such progression correlates with increased accumulation of soluble Aβ42 (Iulita et al., 2014a). Plaque pathology is not apparent in hemizygotes at any age (Leon et al., 2010). In addition to the presence of amyloid plaques, homozygous rats also exhibit strong upregulation large oligomers and of 12 kDa 6E10-immunoreactivity, reflecting the presence of Aβ oligomers (trimers) and/or the C-terminal APP fragment C99 (Fig. 1D).

3.2. NGF and BDNF levels in McGill-R-Thy1-APP rats

To examine changes in the levels of NGF and BDNF across the evolution of Alzheimer-like amyloid pathology, we measured neurotrophin expression in young, pre-plaque, transgenic rats (3–6 months of age), in middle-aged (13–15 months), as well as in old (18–21 months) post-plaque McGill-R-Thy1-APP rats by quantitative qRT-PCR, Western blotting and ELISA.

As expected from human studies (Fahnestock et al., 1996; Goedert et al., 1986; Jette et al., 1994), there was no difference in cortical NGF mRNA expression between APP transgenic rats and non-transgenic (wild type) rats at any time point examined (Fig. 2A–C, *t*-test, $p > 0.05$; 3–6 months, WT $n = 16$ and APP+/+ $n = 13$,

McGill-R-Thy1-APP Transgenic Rats
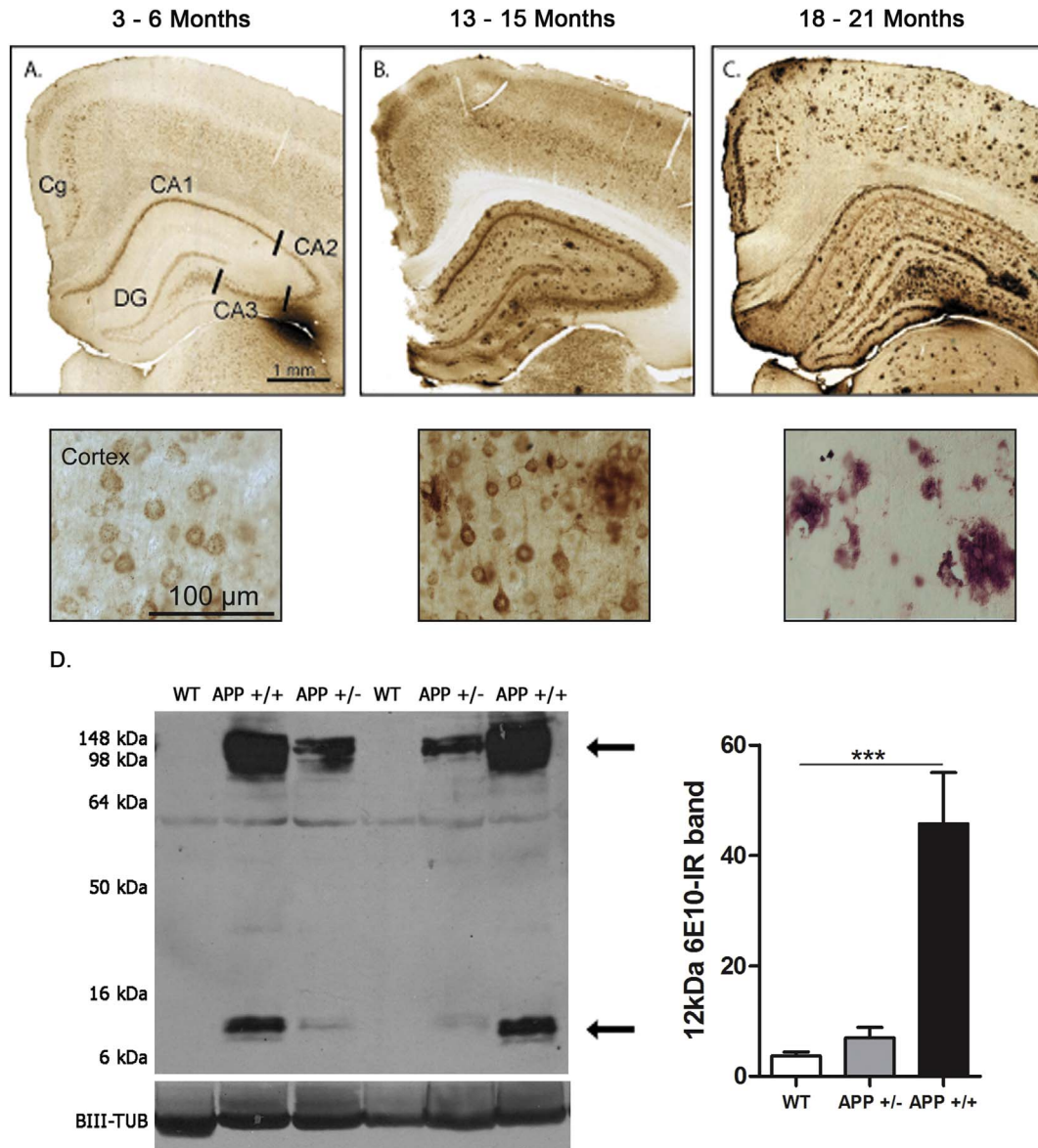
Fig. 1. Evolution of amyloid-β pathology in McGill-R-Thy1-APP transgenic rats. An anti-Aβ mouse monoclonal antibody (McSA1) was used to detect Aβ immunoreactivity. (A) At early stages of amyloid pathology (3–6 months), intraneuronal Aβ accumulated in the cerebral cortex and hippocampus in homozygous transgenic rats. (B) By 13–15 months of age, abundant extracellular amyloid deposits were visible in the hippocampus and fewer in the cortex. (C) As the pathology progressed, old transgenic rats (18–21 months) exhibited abundant amyloid plaque deposition throughout all cortical layers and hippocampal formation. The inserts below panel A, B, and C represent micrographs taken from layer V of the posterior parietal association area. (D) The levels of the 12 kDa-6E10 immunoreactive band (lower arrow) and the ~90–120 kDa immunoreactive band (upper arrow) were significantly elevated in APP homozygote rats, compared to hemizygote and wild-type animals at the post plaque stage (13–15 months). $p < 0.001$, One-way ANOVA and Bonferroni post-test. Graph illustrates mean ± SEM.

13–15 months, WT $n = 13$ and APP +/+ $n = 14$ and 18–21 months, WT $n = 6$ and APP +/+ $n = 7$). However, despite an absence of NGF mRNA deficits, cortical protein levels of proNGF, the precursor to mature NGF, were significantly increased in McGill transgenic rats at all time points analyzed (Fig. 2D–F, *t*-test, D and F, $p < 0.05$ and E, $p < 0.01$; young rats, WT $n = 11$ and APP +/+ $n = 9$, middle-aged rats, WT $n = 20$ and APP +/+ $n = 19$ and old rats, WT $n = 5$ and APP +/+ $n = 5$). In contrast to NGF, BDNF mRNA was downregulated in the cortices of transgenic rats at all ages. BDNF mRNA was significantly downregulated in young, pre-plaque transgenic rats (Fig. 3A, *t*-test $p < 0.05$; WT $n = 10$ and APP +/+ $n = 7$), and there was a trend towards reduced expression of BDNF mRNA levels in middle-aged transgenic animals, compared to non-transgenic littermates (Fig. 3B, *t*-

test $p = 0.14$; WT $n = 19$ and APP +/+ $n = 16$). Further, at post plaque-stages, old transgenic rats (18–21 months) showed significantly decreased expression of BDNF mRNA levels (Fig. 3C, *t*-test $p < 0.05$; WT $n = 7$ and APP +/+ $n = 8$). Protein analysis by Western blotting showed no difference in cortical proBDNF (Fig. 3D–F, *t*-test, $p > 0.05$) or BDNF levels (Fig. 3G–I, *t*-test, $p > 0.05$). These results were corroborated by ELISA in young and middle-aged rats ($p > 0.05$, 3 months: WT $n = 10$; APP +/+ $n = 7$, 13–15 months: WT $n = 14$; APP +/+ $n = 13$; data not shown). Given that BDNF plays an important role in synaptic plasticity and cognition (Greenberg et al., 2009), we investigated whether there was a correlation between BDNF mRNA and cognitive function in young rats. Correlation analysis revealed a significant positive association between BDNF mRNA levels and cognitive
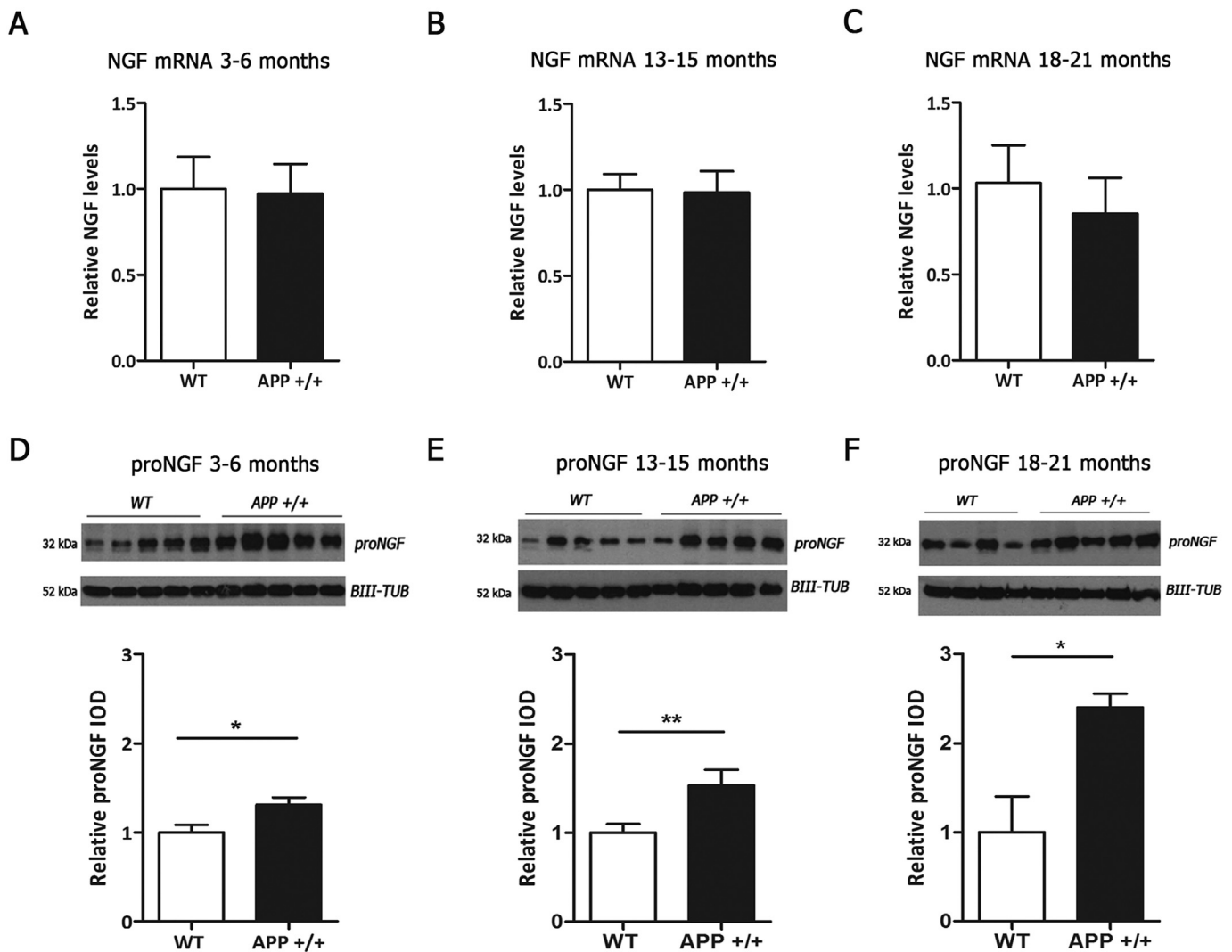
Fig. 2. Analysis of NGF mRNA and proNGF protein expression. (A–C) No difference in cortical NGF mRNA levels between young (3–6 months, WT $n = 16$ and APP $+/+$ $n = 13$) (A), middle-aged (13–15 months, WT $n = 13$ and APP $+/+$ $n = 14$) (B) and old (18–21 months, WT $n = 6$ and APP $+/+$ $n = 7$) (C) transgenic and wild type rats (*t*-test, $p > 0.05$). (D-F) Western blot analysis from cortical brain homogenates revealed significantly increased levels of the 32 kDa proNGF-immunoreactive band in transgenic rats compared to age-matched non-transgenic littermates at all time points analyzed. (D) *$p < 0.05$ (young rats, WT $n = 11$ and APP $+/+$ $n = 9$), (E) ** $p < 0.01$ (middle-aged rats, WT $n = 20$ and APP $+/+$ $n = 19$) and (F) *$p < 0.05$ (old rats, WT $n = 5$ and APP $+/+$ $n = 5$). Densitometry values (IOD) were normalized to β-III tubulin (BIII-Tub). Representative immunoblots per time point are shown.

performance at early stages ($r = 0.626$; $p = 0.001$, Supplementary Fig. 1). Thus, consistent with previous findings of NGF and BDNF deregulation in Alzheimer's disease and Down syndrome (Bruno et al., 2009a; Fahnestock et al., 2001; Fahnestock et al., 1996; Goedert et al., 1986; Iulita et al., 2014b; Michalski and Fahnestock, 2003; Peng et al., 2004; Peng et al., 2005), McGill APP transgenic rats exhibit an accumulation of cortical proNGF without significant changes in NGF mRNA, in parallel with marked reductions in BDNF mRNA expression that correlate with global cognitive deficits.

3.3. Impaired proNGF conversion in McGill-R-Thy1-APP transgenic rats

In order to investigate the origin of the accumulation of the NGF precursor, the levels of key players of the NGF metabolic cascade were analyzed. The expression of tPA, neuroserpin, plasminogen, MMP-9, and TIMP-1 were evaluated in the cerebral cortex of young (3–6 months), middle-aged (13–15 months) and old (18–21 month) transgenic and non-transgenic rats.

We first focused on the NGF maturation pathway, particularly on the enzymes that participate in the maturation of proNGF (Bruno and Cuello, 2006). Quantitative RT-PCR and Western blotting analysis revealed that mRNA and protein levels of tPA were comparable between transgenic and non-transgenic rats at early stages of amyloid pathology (3–6 months, *t*-test $p > 0.05$, WT $n = 16$ and APP $+/+$ $n = 13$ and WT $n = 6$ and APP $+/+$ $n = 8$, Figs. 4A and 5A, respectively). However, as amyloid pathology advanced, APP transgenic rats with amyloid plaque deposition (13–15 and 18–21 months) exhibited a significant decrease in tPA mRNA levels (Fig. 4B and C, *t*-test $p < 0.01$ and $p < 0.05$, 13–15 months WT $n = 15$, and APP $+/+$ $n = 15$ and 18–21 months WT $n = 7$ and APP $+/+$ $n = 8$, respectively). Western blotting showed that protein levels followed the same pattern (Fig. 5B, *t*-test $p < 0.05$; WT $n = 5$ and APP $+/+$ $n = 6$).

There were no differences in protein levels of plasminogen, the zymogen cleaved by tPA into plasmin, between transgenic and non-transgenic rats at early stages of amyloid pathology (Fig. 5C, *t*-test, $p > 0.05$; WT $n = 11$ and APP $+/+$ $n = 9$). In contrast, plasminogen protein levels were significantly elevated at post-plaque stages (Fig. 5D; *t*-test $p < 0.05$; WT $n = 6$ and APP $+/+$ $n = 6$), at time points when reductions in both tPA mRNA and protein levels were observed. This increase in plasminogen protein levels was not due to changes in
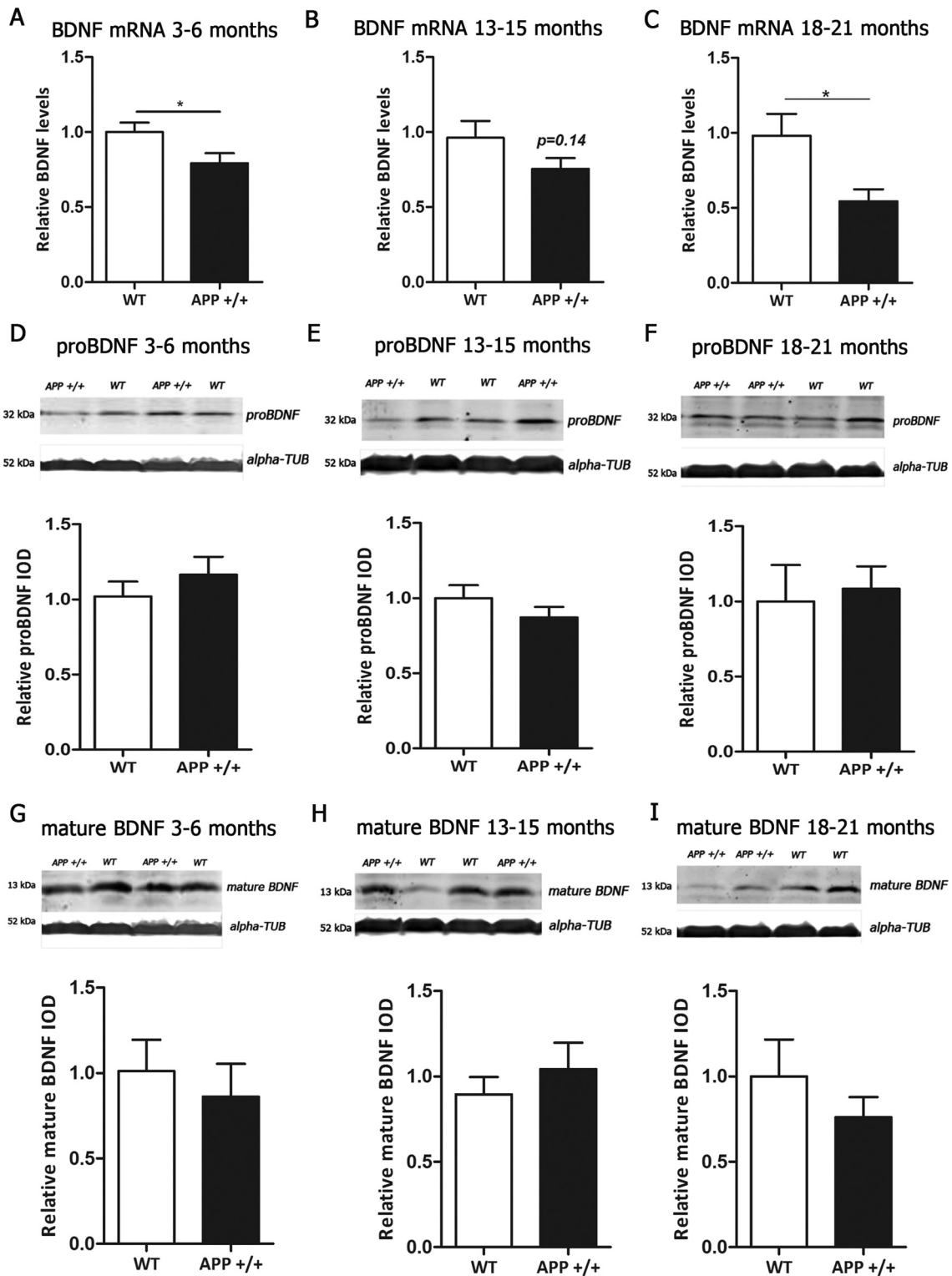
Fig. 3. Analysis of BDNF mRNA and protein. (A–C) mRNA BDNF analysis showed significantly reduced expression in the cortices of young (A) as well as in old-aged transgenic rats (C) and a trend towards reduced mRNA BDNF expression in middle-aged transgenic rats (B) compared to their respective non-transgenic littermates. (A) *p < 0.05 (WT n = 10 and APP +/+ n = 7). (B) t-test, p = 0.14, WT n = 19 and APP +/+ n = 16. (C) *p < 0.05, WT n = 7 and APP +/+ n = 8. (D–I) No differences were detected in cortical proBDNF and mature BDNF protein expression between APP homozygous and wild type rats in young (3–6 months, WT n = 10 and APP +/+ n = 7), middle-aged (13–15 months, WT n = 14 and APP +/+ n = 10) and old animals (18–21 months, WT n = 7 and APP +/+ n = 8) (t-test, p > 0.05). Densitometry values (IOD) were normalized to α-tubulin (α-Tub). Representative immunoblots per time point are shown. Graphs represent mean ± SEM.

plasminogen mRNA expression, which was comparable between APP transgenic rats and controls at all time points investigated (Fig. 4D-F, t-test, p > 0.05; WT n = 16 and APP +/+ n = 13 in young rats; WT n = 15 and APP +/+ n = 13 in middle-aged and WT n = 7 and APP +/+ n = 8 in old rats).

We next investigated whether the changes in plasminogen and tPA were accompanied by differences in the expression of neuroserpin, the endogenous tPA inhibitor (Miranda and Lomas, 2006). Consistent with
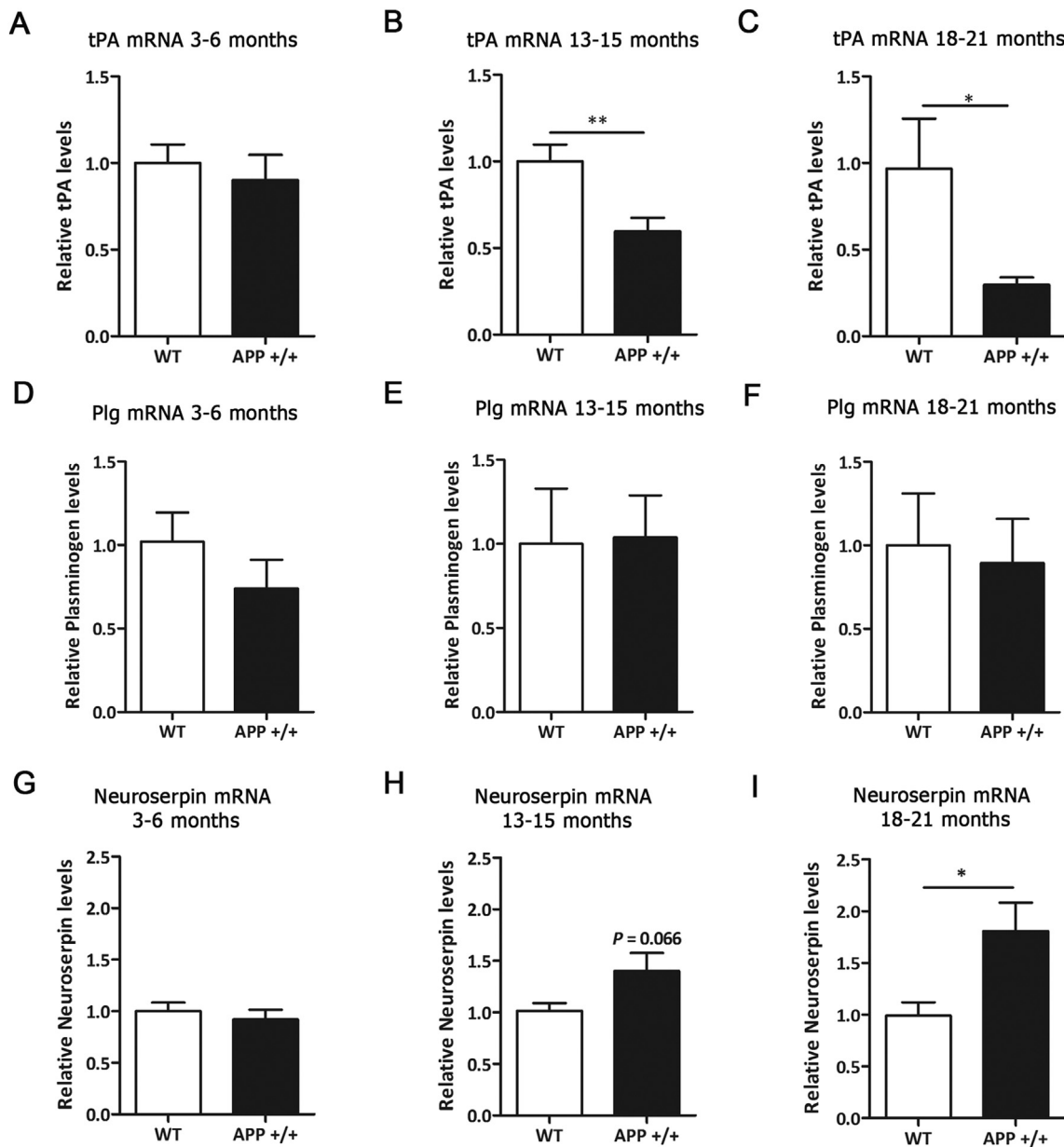
Fig. 4. Alterations in mRNA expression of the enzymes, zymogens and regulators that participate in proNGF maturation. Quantitative PCR analysis of tPA (A–C), plasminogen (D–F) and neuroserpin (G–I) in cortical homogenates from transgenic and wild type rats. (A) No differences in tPA mRNA expression at early stages of the amyloid pathology (3–6 months) (*t*-test, $p > 0.05$, WT $n = 16$ and APP $+/+$ $n = 13$). (B–C) As the amyloid pathology advanced, McGill APP transgenic rats exhibited a significant decrease in tPA mRNA levels compared to wild-type littermates (*t*-test **$p < 0.01$, WT $n = 15$, and APP $+/+$ $n = 15$ and *$p < 0.05$, WT $n = 7$ and APP $+/+$ $n = 8$, respectively). (D–F) No changes in plasminogen mRNA expression at any of the time points investigated (*t*-test, $p > 0.05$, WT $n = 16$ and APP $+/+$ $n = 13$ in young rats; WT $n = 15$ and APP $+/+$ $n = 13$ in middle-aged and WT $n = 7$ and APP $+/+$ $n = 8$ in old rats). (G–I) Neuroserpin mRNA analysis showed no significant differences between transgenic and non-transgenic rats at early time points (3–6 months) (*t*-test, $p > 0.05$, WT $n = 16$ and APP $+/+$ $n = 13$) (G). (H–I) At advanced stages of the amyloid pathology (13–15 and 18–21 months), homozygous transgenic rats exhibited higher neuroserpin mRNA levels compared with their respective non transgenic littermates ($p = 0.066$ WT $n = 13$, and APP $+/+$ $n = 15$ and *$p < 0.01$, wt $n = 6$, and APP $+/+$ $n = 8$). Data are expressed as the mean ± SEM.

the above findings, there was no difference in neuroserpin mRNA and protein levels at the pre-plaque stage (Fig. 4G and 5E, *t*-test, $p > 0.05$; WT $n = 16$ and APP $+/+$ $n = 13$ and WT $n = 6$ and APP $+/+$ $n = 6$, respectively). However, the post-plaque stage was characterized by a strong trend towards upregulation of neuroserpin mRNA levels in middle-aged rats (Fig. 4H; *t*-test, $p = 0.066$; WT $n = 13$, and APP $+/+$ $n = 15$) and by a significant increase in old transgenic rats (Fig. 4I; *t*-test, $p < 0.05$; WT $n = 6$, and APP $+/+$ $n = 8$). These changes were confirmed by Western blotting in middle-aged rats and old rats (Fig. 5F, *t*-test, $p < 0.001$; WT $n = 12$ and APP $+/+$ $n = 8$ and Supplementary Fig. 3).

To investigate whether the *intracellular* processing of proNGF is also

impaired in McGill transgenic rats, we examined the expression of furin, the convertase responsible for the intracellular maturation of proNGF in the secretory pathway (Mowla et al., 1999; Seidah et al., 1996). We found a trend towards decreased mRNA levels of furin in the cortices of young pre-plaque transgenic rats (3–6 months) (Supplementary Fig. 2A, *t*-test, $p = 0.079$; WT $n = 16$ and APP $+/+$ $n = 12$), while levels were significantly decreased in middle-aged (13–15 months) (Supplementary Fig. 2B, *t*-test, $p < 0.01$; WT $n = 14$ and APP $+/+$ $n = 13$) and in old (18–21 months) transgenic rats (Supplementary Fig. 2C, *t*-test, $p < 0.01$; WT $n = 7$ and APP $+/+$ $n = 8$).
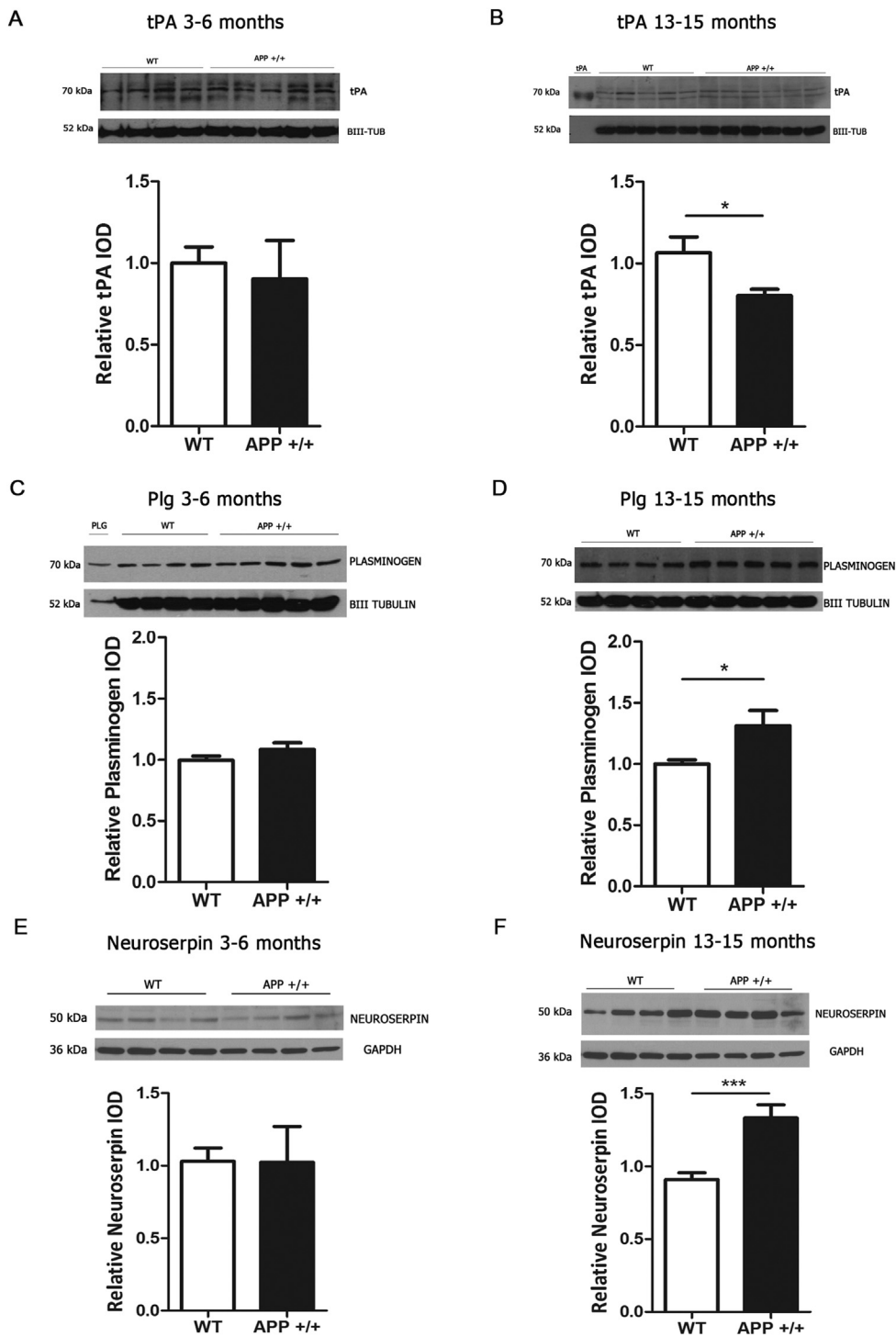
Fig. 5. Alterations in tPA, plasminogen and neuroserpin protein levels. (A–B) Western blotting confirmed the lack of difference in tPA levels between homozygous transgenic rats and wild type rats at early time points ($p > 0.05$ WT $n = 6$ and APP $+/+$ $n = 8$) (A), while revealing a significant tPA downregulation in middle-aged rats (*$p < 0.05$, WT $n = 5$ and APP $+/+$ $n = 6$) (B). Recombinant tPA was used as a positive control (panel B, lane 1). (C) Comparable plasminogen levels between wild type and homozygous transgenic rats at the pre-plaque stage ($p > 0.05$, WT $n = 11$ and APP $+/+$ $n = 9$). (D) Homozygous middle-aged transgenic rats (13–15 months) exhibited a significant increase in plasminogen levels compared to wild type littermates (*$p < 0.05$, WT $n = 6$ and APP $+/+$ $n = 6$). Positive control was a whole cell lysate from B cell lymphoma cells overexpressing plasminogen (panel C, lane 1). (E) No difference in neuroserpin protein levels in young (3–6 months) transgenic rats ($p > 0.05$, WT $n = 6$ and APP $+/+$ $n = 6$) (E), while a significant increase in neuroserpin was evident in homozygous rats at the postplaque stage (13–15 months) (***$p < 0.001$, WT $n = 12$ and APP $+/+$ $n = 8$) (F). Densitometry values (IOD) were normalized to β-III tubulin (BIII-Tub) or GAPDH. Representative immunoblots are shown. Data are expressed as the mean ± SEM.

3.4. Increased MMP-9 activity, a key NGF-degrading protease, in APP transgenic rats

Given the deficits in proNGF maturation, we next investigated whether such changes were accompanied by alterations in the NGF degradation pathway. MMP-9 is a protease responsible for mature NGF degradation (Bruno and Cuello, 2006). MMP-9 mRNA analysis by qRT-PCR did not show significant differences between transgenic and non-transgenic rats at any of the time points investigated (Fig. 6A–B and Supplementary Fig. 3B, *t*-test, $p > 0.05$; young rats WT $n = 16$ and APP $+/+$ $n = 14$, middle-aged transgenic rats, WT $n = 15$ and APP $+/+$ $n = 14$ and old rats WT $n = 7$, APP $+/+$ $n = 8$). Western

blotting further revealed comparable MMP-9 protein expression between homozygous McGill transgenic rats and non-transgenic littermates (Fig. 6C–D, *t*-test, $p > 0.05$; 3–6 months, WT $n = 12$ and APP $+/+$ $n = 13$ and 13–15 months, WT $n = 17$ and APP $+/+$ $n = 14$). When we analyzed the proteolytic activity of MMP-9 by gelatin zymography using cortical homogenates, we found that MMP-9 activity was comparable between transgenic and non-transgenic rats at early stages of amyloid pathology (3–6 months, Fig. 6E, *t*-test $p > 0.05$; WT $n = 8$ and APP $+/+$ $n = 9$). However, there was a significant upregulation of MMP-9 zymogenic activity in middle-aged transgenic rats (13–15 months) compared to non-transgenic littermates (Fig. 6F, *t*-test $p < 0.001$; WT $n = 12$ and APP $+/+$ $n = 8$). MMP-2 activity was
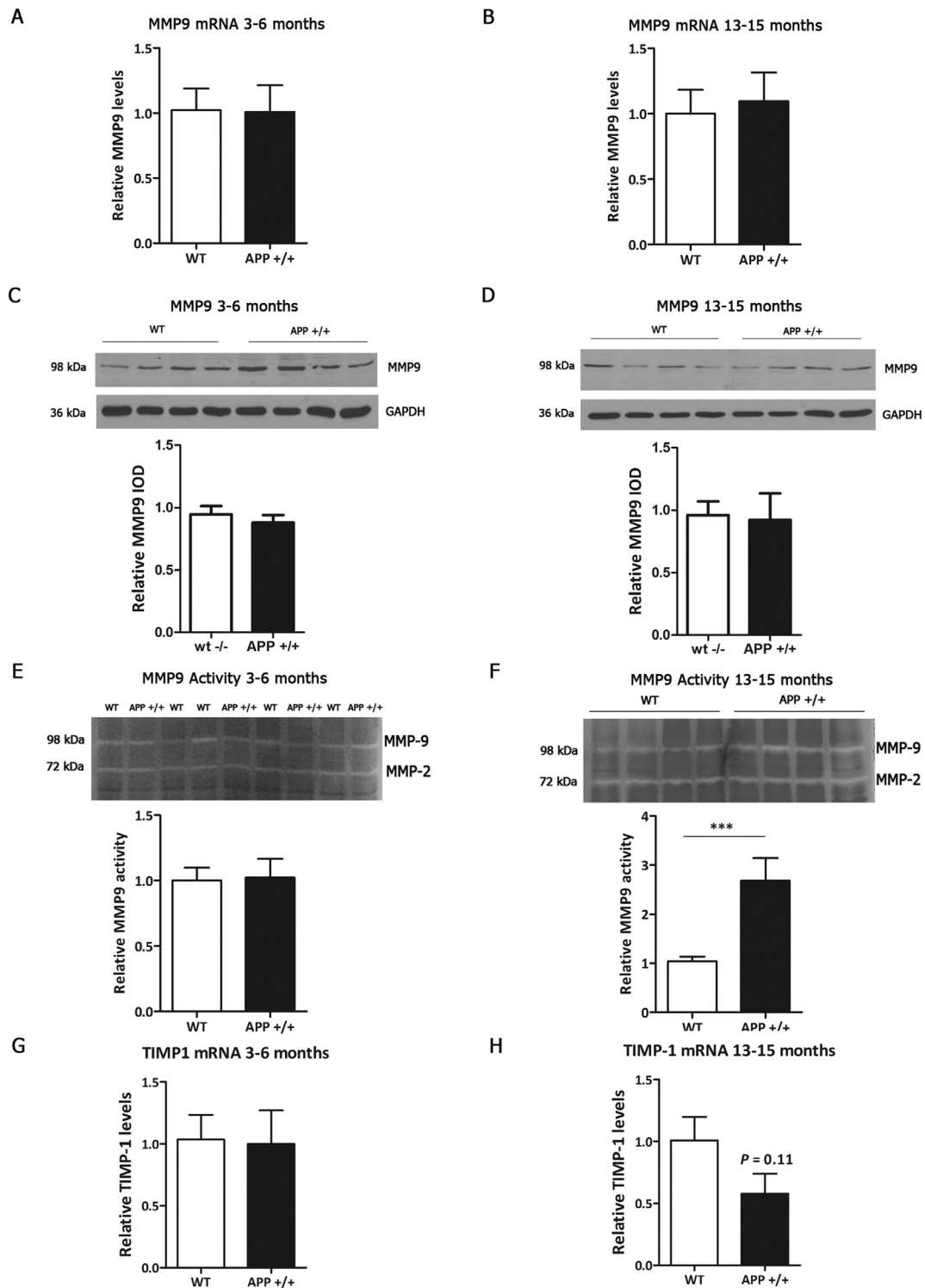
Fig. 6. Analysis of MMP-9 and TIMP-1 expression in McGill transgenic rats. (A–B) No significant differences were detected in cortical MMP-9 mRNA levels in APP homozygous rats, in young (3–6 months, WT $n = 16$ and APP +/+ $n = 14$) (A) or middle-aged transgenic rats (13–15 months, WT $n = 15$ and APP +/+ $n = 14$) (B) compared to non-transgenic littermates (t-test, $p > 0.05$). (C–D) Western blotting revealed comparable MMP-9 protein expression between McGill transgenic rats and non-transgenic littermates either in young (3–6 months, WT $n = 12$ and APP +/+ $n = 13$) and middle-aged rats (13–15 months, WT $n = 17$ and APP +/+ $n = 14$) (t-test, $p > 0.05$) Densitometry values (IOD) were normalized to GAPDH. Representative immunoblots are shown. (E–F) Gelatin zymography of cortex homogenates showed no differences in MMP-9 activity between transgenic and non-transgenic rats at 3–6 months (t-test $p > 0.05$; WT $n = 8$ and APP +/+ $n = 9$) (E). In contrast, middle-aged homozygous transgenic rats exhibited a marked upregulation of MMP-9 activity compared to wild type rats (t-test ***$p < 0.001$, WT $n = 12$ and APP +/+ $n = 8$) (F). MMP-2 activity was comparable between groups ($p > 0.05$), and thus used to normalize MMP-9 activity values. Representative zymograms are shown. (G–H) TIMP-1 mRNA levels were unaltered in young (WT $n = 16$ and APP +/+ $n = 13$) (G) and middle-aged transgenic rats (WT $n = 13$ and APP +/+ $n = 14$) (H) (t-test $p > 0.05$). Data are expressed as the mean ± SEM.

stable between both groups (*t*-test, *p* = 0.20) and thus was used to normalize MMP-9 activity values, as previously done (Bruno et al., 2009a, 2009b).

In light of the increased MMP-9 activity found in McGill transgenic rats, we examined the expression of TIMP-1, its main endogenous inhibitor. Quantitative RT-PCR analysis revealed no differences in TIMP-1 mRNA levels in young or middle-aged transgenic rats (Fig. 6G and H, *t*-test, *p* > 0.05; WT *n* = 16 and APP + / + *n* = 13 and WT *n* = 13 and APP + / + *n* = 14, respectively), although in the latter a clear trend was evident. As the pathology progressed, there continued to be a reduction in TIMP-1 mRNA expression in the cortices of old homozygous transgenic rats, however this difference did not reach statistical significance (*t*-test, *p* = 0.06; WT *n* = 6 and APP + / + *n* = 6) (Supplementary Fig. 3C).

Thus, the upregulation of cortical MMP-9 activity suggests that the extracellular degradation of NGF is enhanced in McGill transgenic rats at advanced stages of Alzheimer-like amyloid pathology. In addition, the absence of changes in TIMP-1 mRNA expression points to other mechanisms responsible for the higher MMP-9 activation in transgenic rats.

3.5. Impact of NGF dysmetabolism on the cholinergic phenotype

The maintenance of the cholinergic phenotype depends on the availability of endogenous NGF, even in the adult CNS. We have previously demonstrated that pharmacological inhibition of proNGF maturation (with the plasmin inhibitor α2-antiplasmin) leads to the atrophy and reduction of pre-existing cortical cholinergic synaptic terminals as well as cognitive deficits (Allard et al., 2012). Therefore, given the observed proNGF accumulation and increased MMP-9 activity in McGill transgenic rats, we sought to investigate whether such changes would impact the density of cholinergic pre-synaptic boutons in this model.

Considering that the alterations in the NGF pathway occurred at the post-plaque stage, we investigated the density of cortical and hippocampal cholinergic pre-synaptic varicosities by immunohistochemistry in 20-month old transgenic rats (Fig. 7). Computer-assisted image analysis quantification revealed a significant reduction in the density of cholinergic boutons both in cortex and in hippocampus of APP rats (*t*-test, *p* < 0.05) (Fig. 7).

4. Discussion

The present study identified differential dysregulation of the neurotrophins NGF and BDNF in the cortices of McGill-R-Thy1-APP transgenic rats, a species closer to humans than mice (Do Carmo and Cuello, 2013). Whereas BDNF mRNA levels were significantly reduced at early stages of amyloid pathology, there were no changes in the expression of NGF mRNA, even at late time points. Furthermore, protein levels of the NGF precursor, proNGF, were increased in McGill transgenic rats despite the normal expression of NGF mRNA. These alterations are in line with human studies on NGF and BDNF levels in Alzheimer's disease cortex (Bruno et al., 2009a; Connor et al., 1997; Fahnestock et al., 2001; Fahnestock et al., 1996; Ferrer et al., 1999; Garzon et al., 2002; Goedert et al., 1986; Hock et al., 2000; Holsinger et al., 2000; Jette et al., 1994; Michalski and Fahnestock, 2003; Pedraza et al., 2005; Peng et al., 2004; Peng et al., 2005; Phillips et al., 1991).

To better understand the opposing differences in NGF mRNA and proNGF protein levels, we examined the expression of key convertases, proteases and regulators of NGF maturation and degradation at time points across the evolution of amyloid pathology. Analysis of cortical homogenates from McGill transgenic rats revealed that proNGF accumulation was accompanied by lower levels of the plasminogen activating protease tPA, and consequently an accumulation of plasminogen, together with up-regulation of neuroserpin at advanced stages of amyloid pathology. These changes indicate a downstream compromise
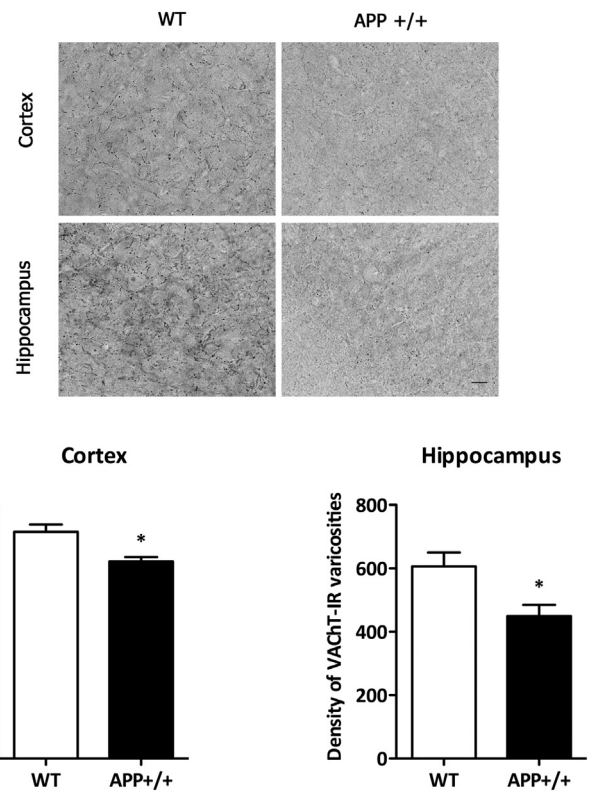

Fig. 7. Impact of NGF-metabolic deficits on the cholinergic phenotype. Quantification of VAChT-labeled cholinergic boutons was done by immunohistochemistry and computer-assisted image analysis. (Upper panel) Representative micrographs illustrating diminished VAChT-labeled cholinergic boutons in cortex and hippocampus of old transgenic rats. (Lower panel) Quantification of VAChT-immunoreactive varicosities expressed as bouton density per imaging field of 30,000 μm². *$p < 0.05$, student *t*-test. Graphs illustrate mean ± SEM. Note the progressive loss of cholinergic presynaptic boutons in both cortex and hippocampus at late stages of AD-like amyloid pathology in McGill APP transgenic rats.

in the levels of cortical active plasmin and therefore, point to a failure in the metabolic loop required for the conversion of proNGF to mature NGF when amyloid plaques are present.

At similar time points, we also detected a significant increase in the zymogenic activity of MMP-9, the main NGF degrading protease (Bruno and Cuello, 2006). The increase in MMP-9 activity suggests that the degradation of mature NGF is greater in McGill APP transgenic rats, thereby further compromising the trophic support of basal forebrain cholinergic neurons. The increase in MMP-9 activity occurred without changes in MMP-9 mRNA or protein expression. We therefore investigated the levels of TIMP-1, which is its endogenous inhibitor. Quantitative RT-PCR analysis revealed a trend towards decreased TIMP-1 mRNA levels in middle-aged transgenic rats, which progressed at advanced stages, although it was not statistically significant. This highlights that other mechanisms besides TIMP-1 downregulation could be responsible for the increased MMP-9 activity observed at the post-plaque stage. For example, pro-inflammatory mediators and reactive oxygen species are known to induce and increase MMP-9 activity (Bugno et al., 1999; Gottschall and Yu, 1995; Gottschall et al., 1995; Gu et al., 2002; Pagenstecher et al., 1998). Interestingly, at post-plaque stages, McGill transgenic rats exhibit increased expression of soluble pro-inflammatory mediators together with a well-established, persistent astrogliosis and recruitment of activated microglia to Aβ-burdened neurons (Hanzel et al., 2014). Thus, it is possible that the increased activation of MMP-9 in transgenic rats is partly due to the combined presence of CNS inflammation and the small reduction in TIMP-1 expression.

Taken together, these results are evidence of a marked

dysregulation of the NGF metabolic pathway in the cerebral cortex of the McGill-R-Thy1-APP transgenic rats, similar to that previously found in the brains of Alzheimer's disease patients (Bruno et al., 2009a) and in demented individuals with Down syndrome (Iulita et al., 2014b), as recently reviewed (Iulita and Cuello, 2014; Iulita and Cuello, 2016). Defective NGF metabolism may explain the increase in proNGF in the absence of changes in NGF mRNA. Consistent with our study, 3xTg-AD mice exhibit proNGF accumulation in cortex and cholinergic deficits, evidenced by reduced ChAT activity in the hippocampus and in the medial septum (Perez et al., 2011).

The changes in proNGF proteases and regulators were detected in middle-aged (13–15 months) and old (18–21 months) McGill APP transgenic rats, when extensive intracellular Aβ and extracellular amyloid plaques are present. However, it is important to note this does not necessarily rule out the possibility that changes in NGF metabolism appear at early pre-clinical stages in human pathology. Individuals with MCI present a very similar neuropathological phenotype to that of Alzheimer patients, with abundant amyloid plaque deposits and neurofibrillary tangles (which are absent in this transgenic model), as well as increased proNGF (Peng et al., 2004) and MMP-9 activity (Bruno et al., 2009b). Therefore, although NGF deficits appeared at late stages of amyloid pathology in the rat, it is likely that such changes manifest earlier in humans, perhaps even prior to MCI.

Despite an absence of changes in tPA, plasminogen, and neuroserpin at the pre-plaque stage, proNGF was found to be increased at this early time point (mainly mediated by an increase in 6 month-old rats). These findings raise the possibility that other processes could also participate in proNGF accumulation. In line with this, Scott and colleagues have demonstrated that increased NGF-like immunoreactivity in cortex and hippocampus of Alzheimer's disease patients is coupled with decreased NGF-like immunoreactivity in nucleus basalis, suggesting that impaired retrograde transport may be responsible (Scott et al., 1995). In genetic models of Down syndrome, which exhibit APP triplication, a reduction in the transport of radiolabeled NGF (injected into the hippocampus and measured in the septum) is evident in parallel with cholinergic neuron degeneration (Salehi et al., 2006). Given that the retrograde flux of fluorolabeled proNGF in cultured sensory neurons is similar -albeit initially slower- to that of mature NGF (De Nadai et al., 2016), one could hypothesize that impaired retrograde transport could also contribute to proNGF accumulation. This remains to be tested *in vivo* in the context of basal forebrain cholinergic neuron degeneration. Furthermore, other proteases besides plasmin may participate in proNGF maturation, for example, proprotein convertases (Mowla et al., 1999). Thus, we investigated whether the early rise in proNGF may be due to a failure in its intracellular furin-mediated conversion. Although we found a trend for a reduction in furin mRNA levels in young rats, these changes were only significant at advanced pathological stages. This finding strengthens the idea that other intracellular or extracellular proteases, which may be released with proNGF in an activity-dependent manner, could participate in proNGF maturation, warranting future studies on NGF processing and release *ex vivo*.

The biological relevance of dysregulated neurotrophin metabolism in amyloid pathologies is best understood in terms of the trophic dependency of CNS cholinergic neurons. First, since BDNF is known to regulate synaptic plasticity and cholinergic enzyme expression in rat septal neurons (Klein et al., 1999; Knusel et al., 1991; Nonomura and Hatanaka, 1992), decreased BDNF expression early in the disease process may compromise cholinergic synaptic function. Second, defective maturation of proNGF would progressively deprive forebrain cholinergic neurons of trophic support and thus, further impact the maintenance of their cholinergic phenotype.

Additional studies will be required to differentiate the effects of decreased BDNF expression and increased proNGF on cholinergic synapses, particularly at younger ages. Nevertheless, the results of this study are in line with the finding that the localized cortical inhibition of plasmin activity (precluding proNGF maturation) results in a loss of

cortical cholinergic synaptic boutons in the treated area (Allard et al., 2012). They are also in agreement with the observation that short-term inhibition of tPA activity is sufficient to markedly lower the CNS levels of endogenous NGF and to increase proNGF levels in the cerebral cortex of naïve rats (Bruno and Cuello, 2006). As NGF and BDNF are compromised in amyloid pathologies (Bruno et al., 2009a; Connor et al., 1997; Ferrer et al., 1999; Garzon et al., 2002; Hock et al., 2000; Holsinger et al., 2000; Iulita et al., 2014b; Michalski and Fahnestock, 2003; Peng et al., 2005; Phillips et al., 1991), and as proNGF and BDNF levels can be regulated by Aβ oligomers (Bruno et al., 2009a; Francis et al., 2012; Garzon and Fahnestock, 2007), we pose the hypothesis that Aβ-amyloidosis is sufficient to impair BDNF expression and NGF metabolism and to negatively affect the basal forebrain cholinergic synapse and phenotype. Independently of the above, there is also a direct action of Aβ-amyloid peptides on forebrain cholinergic neurons that could explain their vulnerability in Alzheimer's disease. For example, in *in vitro* slice preparations Aβ inhibits acetylcholine release and choline uptake (Kar et al., 1998; Kar et al., 1996), which could affect cholinergic synapses. Indeed, in rodent models of amyloid pathology, up-regulation of cholinergic synapses is observed at pre-plaque stages followed by a decrease (Bell et al., 2006; Hu et al., 2003; Wong et al., 1999). This is in line with the cholinergic compromise in human amyloid pathology, where increased ChAT activity occurs early (in MCI) (DeKosky et al., 2002) followed by a decrease in Alzheimer's disease brains (Bowen et al., 1976; Davies, 1979; Davies and Maloney, 1976; Perry et al., 1977; Reisine et al., 1978; Sims et al., 1983).

Although reduced supply of mature NGF due to proNGF dysmetabolism may directly compromise basal forebrain cholinergic neuronal viability, an additional mechanism further contributing to their degeneration in Alzheimer's disease could be an imbalance in NGF receptors. The receptor for NGF (TrkA) progressively decreases in MCI and Alzheimer's disease (Counts et al., 2004; Ginsberg et al., 2006; Mufson et al., 2012; Mufson et al., 2000). The causes for this progressive loss remain elusive; however given that TrkA mRNA expression is sustained by the presence of NGF (Figueiredo et al., 1995; Venero et al., 1994), such reduction in TrkA levels may be attributed to the compromise of the NGF metabolic pathway (*i.e.* impaired proNGF maturation). As TrkA decreases, proNGF accumulation occurs in the presence of elevated levels of p75NTR (Mufson et al., 2007). It has been demonstrated *in vitro* that proNGF biological activity switches from neurotrophic (Buttigieg et al., 2007; Clewes et al., 2008; Fahnestock et al., 2004) to apoptotic in embryonic cells as the balance of receptors shifts from TrkA to p75NTR (Masoudi et al., 2009). Thus, in the adult human brain, where proNGF is the dominant form of NGF detected (Fahnestock et al., 2001), cholinergic degeneration may coincide with impaired proNGF metabolism, reduced binding to TrkA and increased binding to p75NTR.

It is interesting to note that while transgenic rats exhibit no change in NGF mRNA even with advanced pathology; BDNF mRNA expression is reduced, starting at very early stages of intraneuronal Aβ accumulation, when no plaques are present. These results are consistent with *in vitro* data demonstrating that soluble oligomeric, but not fibrillar, Aβ down-regulates BDNF (Garzon and Fahnestock, 2007), and with transgenic mouse studies demonstrating BDNF downregulation prior to plaque formation (Francis et al., 2012). These results also support the concept of toxic intracellular Aβ effects on CNS homeostasis, demonstrating that extracellular Aβ is not necessary for BDNF loss *in vivo*. Consistent with human studies (Buchman et al., 2016; Peng et al., 2005), reductions in BDNF mRNA correlated with cognitive deficits. For proNGF, an inverse relation has been reported between its cortical levels and cognitive scores in MCI and Alzheimer's disease (Peng et al., 2004); and in Down syndrome, the yearly rise in plasma proNGF correlated with progressive cognitive decline (Iulita et al., 2016).

The decrease in BDNF mRNA preceded the deregulation of the NGF metabolic pathway and the decline in VAChT-immunoreactive boutons, which occur at the post-plaque stage. It should be noted that in some
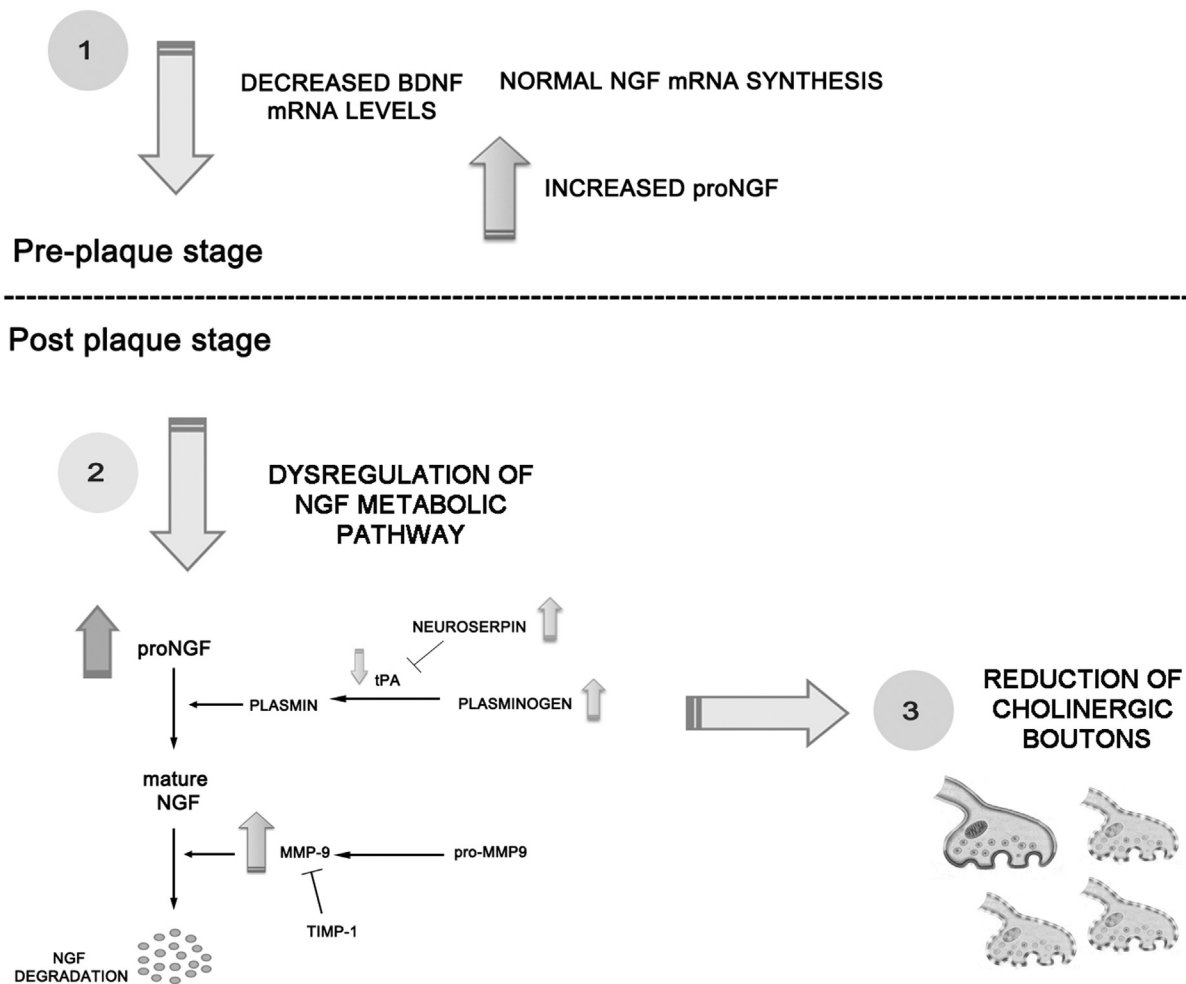
Fig. 8. Schematic representation of NGF and BDNF alterations in McGill-R-Thy1-APP transgenic rats. Before amyloid plaques appear (pre-plaque stage), there is a significant down-regulation of BDNF mRNA and an increase in proNGF protein in the cortices of young APP rats, while the levels of NGF mRNA are normal (1). As the amyloid pathology advances (post-plaque stage), an NGF metabolic compromise became evident in middle-aged and old rats (2). Briefly, the dysregulation of the NGF metabolic pathway was characterized by reduced expression of tPA and higher levels of plasminogen and neuroserpin, suggesting an impaired maturation of proNGF and hence its accumulation. The availability of NGF was further compromised by the increased activity of MMP-9, its main degrading protease. No significant changes in the expression of its endogenous inhibitor TIMP-1 were detected in this model, although a trend for a reduction in TIMP-1 mRNA was evident. The biological significance of these alterations was reflected by the downregulation of cortical and hippocampal cholinergic boutons at advanced stages of amyloid pathology (3). Arrows indicate the dysregulation of BDNF mRNA, proNGF protein and of the enzymes participating in NGF maturation and degradation.

transgenic lines (*e.g.* APP23 mice) an increase in BDNF transcript and protein has been reported in the vicinity of amyloid plaques (Burbach et al., 2004; Schulte-Herbruggen et al., 2008). These discrepancies can be due to the fact that genetic charge and burden of amyloid pathology may not be comparable between models and across species. The current rat transgenic model has the lowest genetic charge compared to other models of cerebral amyloidosis, which are mainly mice. An alternative explanation could be a biphasic deregulation of BDNF transcript and protein throughout the evolution of the human amyloid pathology, as has been seen with cholinergic synapses.

Despite the decrease in BDNF mRNA, no loss of mature BDNF or proBDNF protein was found. Given that the reduction in BDNF mRNA is relatively small in this model compared to the approximately 70% reduction in late-stage Alzheimer's disease (Holsinger et al., 2000), it is possible that this is not sufficient to impact BDNF protein levels. Previous work comparing BDNF mRNA reductions in various transgenic mouse models (Peng et al., 2009) implicated high-molecular-weight oligomers in BDNF downregulation. The McGill-R-Thy1-APP rat model exhibits predominantly trimers rather than larger oligomers (Do Carmo and Cuello, 2013), which may account for the less profound effect on BDNF mRNA. Alternatively, the techniques employed may have been unable to detect small reductions in BDNF protein content in transgenic

rats. In a study using human AD tissue, BDNF mRNA measured by the highly sensitive qRT-PCR assay used here detected a 34-fold difference between the lowest and highest tested samples, whereas BDNF ELISA detected only a 4-fold range in BDNF protein levels in the same samples (Michalski et al., 2015). In addition, AD post-mortem studies suggest that mature BDNF is present in lower amounts in the cortex than proBDNF and decreases much more sharply than proBDNF in the prodromal stages of AD (Peng et al., 2005). Mature BDNF can be formed extracellularly as a result of activity-dependent secretion of proBDNF and tPA (*via* the proteolytic action of plasmin) (Pang et al., 2004). Therefore, it is likely that the reduction in tPA and associated dysmetabolism in plasmin and neuroserpin shown here may also decrease maturation of BDNF, which would lead to higher levels of proBDNF and lower mature BDNF. On the other hand, in contrast to NGF which is degraded by MMP-9 (Bruno and Cuello, 2006), MMP-9 converts proBDNF to mature BDNF (Mizoguchi et al., 2011). Therefore, the increase in MMP-9 seen here may increase the production of mature BDNF, negating any decrease caused by loss of tPA.

Multiple pathways are responsible for downregulation of BDNF in Alzheimer's disease. Only four of the 17 transcripts expressed in the human cortex are downregulated in Alzheimer's disease, specifically transcripts I, II, IV and VI (Garzon et al., 2002). Soluble, oligomeric Aβ,

but not the fibrillar Aβ found in plaques, downregulates BDNF transcript IV, the transcript that accounts for over half of the BDNF expressed in cortical tissues (Garzon and Fahnestock, 2007). Transcript IV is therefore the major contributor to BDNF loss in Alzheimer's disease. Aβ downregulates BDNF transcript IV *via* a variety of mechanisms converging on the transcription factor CREB (cyclic AMP response element binding protein). In *in vitro* studies, differentiated human neuroblastoma cells treated with soluble oligomeric Aβ exhibit a reduction of CREB transcription, which in turn impacts BDNF expression (Rosa and Fahnestock, 2015). Consistent with the above, a recent *in vivo* study in young, pre-plaque McGill APP transgenic rats revealed that deficits in associative learning were accompanied by reduced nuclear translocation and CRE-promoter occupancy of CRTC1, the CREB coactivator, together with reduced expression of synaptic plasticity genes activated by CREB, such as BDNF, Arc, c-fos and Egr1 (Wilson et al., 2016; Wilson et al., 2017). Studies in other transgenic models and in human Alzheimer brains further support a role for Aβ in disrupting CREB co-activation and CREB-regulated transcription of memory-related genes (*e.g.* BDNF) and hence cognition (Espana et al., 2010; Parra-Damas et al., 2017; Parra-Damas et al., 2014).

In closing, McGill APP transgenic rats exhibit differential dysregulation in NGF and BDNF neurotrophins. At early stages, intraneuronal Aβ leads to significant reductions in BDNF mRNA expression, which correlate with learning and memory deficits. At later stages, deficits in the NGF metabolic pathway could explain the paradoxical upregulation of proNGF in the absence of changes in NGF mRNA, similar to that observed in Alzheimer's disease and Down syndrome (Iulita and Cuello, 2014; Iulita and Cuello, 2016; Jette et al., 1994). Compromised BDNF expression and NGF metabolism would negatively affect the cholinergic basal forebrain phenotype, resulting in reduction of pre-existing cortical cholinergic synapses, a phenotypic feature tightly regulated by the supply of *endogenous* brain NGF (Debeir et al., 1999). A schematic representation summarizing these alterations is depicted in Fig. 8. Thus, McGill APP transgenic rats offer a suitable *in vivo* platform to test novel therapeutic approaches aimed at correcting NGF-metabolic deficits and/or BDNF loss in the central nervous system.

Supplementary data to this article can be found online at http://dx.doi.org/10.1016/j.nbd.2017.08.019.

Author contributions

MFI, MBBM, MAB, MF and ACC designed the study. MFI, MBB, RP, LFA, SDC, SA, BM, ENW and AD generated and analyzed the experimental data. MFI, MBB, MAB, MF and ACC wrote the manuscript. All authors read and edited the manuscript.

Conflicts of interest

The authors have nothing to disclose.

References

Allard, S., et al., 2012. Impact of the NGF maturation and degradation pathway on the cortical cholinergic system phenotype. J. Neurosci. 32, 2002–2012.
Allen, S.J., Dawbarn, D., 2006. Clinical relevance of the neurotrophins and their receptors. Clin. Sci. (Lond.) 110, 175–191.
Bartus, R.T., et al., 1982. The cholinergic hypothesis of geriatric memory dysfunction. Science 217, 408–414.
Bell, K.F., et al., 2006. The amyloid pathology progresses in a neurotransmitter-specific manner. Neurobiol. Aging 27, 1644–1657.
Bibel, M., Barde, Y.A., 2000. Neurotrophins: key regulators of cell fate and cell shape in the vertebrate nervous system. Genes Dev. 14, 2919–2937.
Billings, L.M., et al., 2005. Intraneuronal Abeta causes the onset of early Alzheimer's disease-related cognitive deficits in transgenic mice. Neuron 45, 675–688.
Bowen, D.M., et al., 1976. Neurotransmitter-related enzymes and indices of hypoxia in senile dementia and other abiotrophies. Brain 99, 459–496.
Bruno, M.A., Cuello, A.C., 2006. Activity-dependent release of precursor nerve growth factor, conversion to mature nerve growth factor, and its degradation by a protease cascade. Proc. Natl. Acad. Sci. U. S. A. 103, 6735–6740.
Bruno, M.A., et al., 2009a. Amyloid beta-induced nerve growth factor dysmetabolism in Alzheimer disease. J. Neuropathol. Exp. Neurol. 68, 857–869.
Bruno, M.A., et al., 2009b. Increased matrix metalloproteinase 9 activity in mild cognitive impairment. J. Neuropathol. Exp. Neurol. 68, 1309–1318.
Buchman, A.S., et al., 2016. Higher brain BDNF gene expression is associated with slower cognitive decline in older adults. Neurology 86, 735–741.
Bugno, M., et al., 1999. Reprogramming of TIMP-1 and TIMP-3 expression profiles in brain microvascular endothelial cells and astrocytes in response to proinflammatory cytokines. FEBS Lett. 448, 9–14.
Burbach, G.J., et al., 2004. Induction of brain-derived neurotrophic factor in plaque-associated glial cells of aged APP23 transgenic mice. J. Neurosci. 24, 2421–2430.
Burns, A., Illiffe, S., 2009. BMJ. http://dx.doi.org/10.1136/bmj.b158.
Buttigieg, H., et al., 2007. Neurotrophic activity of proNGF in vivo. Exp. Neurol. 204, 832–835.
Cleary, J.P., et al., 2005. Natural oligomers of the amyloid-beta protein specifically disrupt cognitive function. Nat. Neurosci. 8, 79–84.
Clewes, O., et al., 2008. Human ProNGF: biological effects and binding profiles at TrkA, P75NTR and sortilin. J. Neurochem. 107, 1124–1135.
Connor, B., et al., 1997. Brain-derived neurotrophic factor is reduced in Alzheimer's disease. Brain Res. Mol. Brain Res. 49, 71–81.
Côté, S.L., et al., 1994. Current Protocols for Light Microscopy Immunocytochemistry. John Wiley and Sons, Chichester.
Counts, S.E., et al., 2004. Reduction of cortical TrkA but not p75(NTR) protein in early-stage Alzheimer's disease. Ann. Neurol. 56, 520–531.
Coyle, J.T., et al., 1983. Alzheimer's disease: a disorder of cortical cholinergic innervation. Science 219, 1184–1190.
Cuello, A.C., 1996. Effects of trophic factors on the CNS cholinergic phenotype. Prog. Brain Res. 109, 347–358.
Cuello, A.C., Bruno, M.A., 2007. The failure in NGF maturation and its increased degradation as the probable cause for the vulnerability of cholinergic neurons in Alzheimer's disease. Neurochem. Res. 32, 1041–1045.
Davies, P., 1979. Neurotransmitter-related enzymes in senile dementia of the Alzheimer type. Brain Res. 171, 319–327.
Davies, P., Maloney, A.J., 1976. Selective loss of central cholinergic neurons in Alzheimer's disease. Lancet 2, 1403.
De Nadai, T., et al., 2016. Precursor and mature NGF live tracking: one versus many at a time in the axons. Sci Rep 6, 20272.
Debeir, T., et al., 1999. A nerve growth factor mimetic TrkA antagonist causes withdrawal of cortical cholinergic boutons in the adult rat. Proc. Natl. Acad. Sci. U. S. A. 96, 4067–4072.
DeKosky, S.T., Scheff, S.W., 1990. Synapse loss in frontal cortex biopsies in Alzheimer's disease: correlation with cognitive severity. Ann. Neurol. 27, 457–464.
DeKosky, S.T., et al., 2002. Upregulation of choline acetyltransferase activity in hippocampus and frontal cortex of elderly subjects with mild cognitive impairment. Ann. Neurol. 51, 145–155.
Do Carmo, S., Cuello, A.C., 2013. Modeling Alzheimer's disease in transgenic rats. Mol. Neurodegener. 8, 37.
Drachman, D.A., Leavitt, J., 1974. Human memory and the cholinergic system. A relationship to aging? Arch. Neurol. 30, 113–121.
Dubois, B., et al., 2016. Preclinical Alzheimer's disease: definition, natural history, and diagnostic criteria. Alzheimers Dement. 12, 292–323.
Echeverria, V., et al., 2004. Altered mitogen-activated protein kinase signaling, tau

hyperphosphorylation and mild spatial learning dysfunction in transgenic rats expressing the beta-amyloid peptide intracellularly in hippocampal and cortical neurons. Neuroscience 129, 583–592.

Eikelenboom, P., et al., 1998. Inflammation and Alzheimer's disease: relationships between pathogenic mechanisms and clinical expression. Exp. Neurol. 154, 89–98.

Espana, J., et al., 2010. beta-Amyloid disrupts activity-dependent gene transcription required for memory through the CREB coactivator CRTC1. J. Neurosci. 30, 9402–9410.

Etienne, P., et al., 1986. Nucleus basalis neuronal loss, neuritic plaques and choline acetyltransferase activity in advanced Alzheimer's disease. Neuroscience 19, 1279–1291.

Fahnestock, M., et al., 1996. Nerve growth factor mRNA and protein levels measured in the same tissue from normal and Alzheimer's disease parietal cortex. Brain Res. Mol. Brain Res. 42, 175–178.

Fahnestock, M., et al., 2001. The precursor pro-nerve growth factor is the predominant form of nerve growth factor in brain and is increased in Alzheimer's disease. Mol. Cell. Neurosci. 18, 210–220.

Fahnestock, M., et al., 2004. The nerve growth factor precursor proNGF exhibits neurotrophic activity but is less active than mature nerve growth factor. J. Neurochem. 89, 581–592.

Ferrer, I., et al., 1999. BDNF and full-length and truncated TrkB expression in Alzheimer disease. Implications in therapeutic strategies. J. Neuropathol. Exp. Neurol. 58, 729–739.

Ferretti, M.T., et al., 2011. Transgenic mice as a model of pre-clinical Alzheimer's disease. Curr. Alzheimer Res. 8, 4–23.

Ferretti, M.T., et al., 2012. Intracellular Abeta-oligomers and early inflammation in a model of Alzheimer's disease. Neurobiol. Aging 33, 1329–1342.

Figueiredo, B.C., et al., 1995. Differential expression of p140trk, p75NGFR and growth-associated phosphoprotein-43 genes in nucleus basalis magnocellularis, thalamus and adjacent cortex following neocortical infarction and nerve growth factor treatment. Neuroscience 68, 29–45.

Francis, B.M., et al., 2012. Object recognition memory and BDNF expression are reduced in young TgCRND8 mice. Neurobiol. Aging 33, 555–563.

Galeano, P., et al., 2014. Longitudinal analysis of the behavioral phenotype in a novel transgenic rat model of early stages of Alzheimer's disease. Front. Behav. Neurosci. 8, 321.

Garzon, D.J., Fahnestock, M., 2007. Oligomeric amyloid decreases basal levels of brain-derived neurotrophic factor (BDNF) mRNA via specific downregulation of BDNF transcripts IV and V in differentiated human neuroblastoma cells. J. Neurosci. 27, 2628–2635.

Garzon, D., et al., 2002. A new brain-derived neurotrophic factor transcript and decrease in brain-derived neurotrophic factor transcripts 1, 2 and 3 in Alzheimer's disease parietal cortex. J. Neurochem. 82, 1058–1064.

Ginsberg, S.D., et al., 2006. Down regulation of trk but not p75NTR gene expression in single cholinergic basal forebrain neurons mark the progression of Alzheimer's disease. J. Neurochem. 97, 475–487.

Goedert, M., et al., 1986. Nerve growth factor mRNA in peripheral and central rat tissues and in the human central nervous system: lesion effects in the rat brain and levels in Alzheimer's disease. Brain Res. 387, 85–92.

Goedert, M., et al., 1988. Cloning and sequencing of the cDNA encoding a core protein of the paired helical filament of Alzheimer disease: identification as the microtubule-associated protein tau. Proc. Natl. Acad. Sci. U. S. A. 85, 4051–4055.

Gottschall, P.E., Yu, X., 1995. Cytokines regulate gelatinase A and B (matrix metalloproteinase 2 and 9) activity in cultured rat astrocytes. J. Neurochem. 64, 1513–1520.

Gottschall, P.E., et al., 1995. Increased production of gelatinase B (matrix metalloproteinase-9) and interleukin-6 by activated rat microglia in culture. J. Neurosci. Res. 42, 335–342.

Grant, S.M., et al., 2000. Abeta immunoreactive material is present in several intracellular compartments in transfected, neuronally differentiated, P19 cells expressing the human amyloid beta-protein precursor. J. Alzheimers Dis. 2, 207–222.

Greenberg, M.E., et al., 2009. New insights in the biology of BDNF synthesis and release: implications in CNS function. J. Neurosci. 29, 12764–12767.

Grundke-Iqbal, I., et al., 1986. Abnormal phosphorylation of the microtubule-associated protein tau (tau) in Alzheimer cytoskeletal pathology. Proc. Natl. Acad. Sci. U. S. A. 83, 4913–4917.

Gu, Z., et al., 2002. S-nitrosylation of matrix metalloproteinases: signaling pathway to neuronal cell death. Science 297, 1186–1190.

Hanzel, C.E., et al., 2014. Neuronal driven pre-plaque inflammation in a transgenic rat model of Alzheimer's disease. Neurobiol. Aging 35, 2249–2262.

Hock, C., et al., 2000. Region-specific neurotrophin imbalances in Alzheimer disease: decreased levels of brain-derived neurotrophic factor and increased levels of nerve growth factor in hippocampus and cortical areas. Arch. Neurol. 57, 846–851.

Holsinger, R.M., et al., 2000. Quantitation of BDNF mRNA in human parietal cortex by competitive reverse transcription-polymerase chain reaction: decreased levels in Alzheimer's disease. Brain Res. Mol. Brain Res. 76, 347–354.

Hu, L., et al., 2003. The impact of Abeta-plaques on cortical cholinergic and non-cholinergic presynaptic boutons in alzheimer's disease-like transgenic mice. Neuroscience 121, 44, 421–426.

Iulita, M.F., Cuello, A.C., 2014. Nerve growth factor metabolic dysfunction in Alzheimer's disease and down syndrome. Trends Pharmacol. Sci. 35, 338–348.

Iulita, M.F., Cuello, A.C., 2016. The NGF metabolic pathway in the CNS and its dysregulation in down syndrome and Alzheimer's disease. Curr. Alzheimer Res. 13, 53–67.

Iulita, M.F., et al., 2014a. Intracellular Abeta pathology and early cognitive impairments in a transgenic rat overexpressing human amyloid precursor protein: a multidimensional study. Acta Neuropathol. Commun. 2, 61.

Iulita, M.F., et al., 2014b. Nerve growth factor metabolic dysfunction in Down's syndrome

brains. Brain 137, 860–872.

Iulita, M.F., et al., 2016. An Inflammatory and Trophic Disconnect Biomarker Profile Revealed in Down Syndrome Plasma: Relation to Cognitive Decline and Longitudinal Evaluation. Alzheimers Dement.

Je, H.S., et al., 2012. Role of pro-brain-derived neurotrophic factor (proBDNF) to mature BDNF conversion in activity-dependent competition at developing neuromuscular synapses. Proc. Natl. Acad. Sci. U. S. A. 109, 15924–15929.

Jette, N., et al., 1994. NGF mRNA is not decreased in frontal cortex from Alzheimer's disease patients. Brain Res. Mol. Brain Res. 25, 242–250.

Jin, M., et al., 2011. Soluble amyloid beta-protein dimers isolated from Alzheimer cortex directly induce Tau hyperphosphorylation and neuritic degeneration. Proc. Natl. Acad. Sci. U. S. A. 108, 5819–5824.

Kar, S., et al., 1996. Beta-amyloid-related peptides inhibit potassium-evoked acetylcholine release from rat hippocampal slices. J. Neurosci. 16, 1034–1040.

Kar, S., et al., 1998. Amyloid beta-peptide inhibits high-affinity choline uptake and acetylcholine release in rat hippocampal slices. J. Neurochem. 70, 2179–2187.

Klein, R.L., et al., 1999. Long-term actions of vector-derived nerve growth factor or brain-derived neurotrophic factor on choline acetyltransferase and Trk receptor levels in the adult rat basal forebrain. Neuroscience 90, 815–821.

Knusel, B., et al., 1991. Promotion of central cholinergic and dopaminergic neuron differentiation by brain-derived neurotrophic factor but not neurotrophin 3. Proc. Natl. Acad. Sci. U. S. A. 88, 961–965.

Lambert, M.P., et al., 1998. Diffusible, nonfibrillar ligands derived from Abeta1-42 are potent central nervous system neurotoxins. Proc. Natl. Acad. Sci. U. S. A. 95, 6448–6453.

Leon, W.C., et al., 2010. A novel transgenic rat model with a full Alzheimer's-like amyloid pathology displays pre-plaque intracellular amyloid-beta-associated cognitive impairment. J. Alzheimers Dis. 20, 113–126.

Lesne, S., et al., 2006. A specific amyloid-beta protein assembly in the brain impairs memory. Nature 440, 352–357.

Masoudi, R., et al., 2009. Biological activity of nerve growth factor precursor is dependent upon relative levels of its receptors. J. Biol. Chem. 284, 18424–18433.

McGeer, P.L., et al., 1987. Reactive microglia in patients with senile dementia of the Alzheimer type are positive for the histocompatibility glycoprotein HLA-DR. Neurosci. Lett. 79, 195–200.

Mesulam, M.M., et al., 1983. Central cholinergic pathways in the rat: an overview based on an alternative nomenclature (Ch1-Ch6). Neuroscience 10, 1185–1201.

Michalski, B., Fahnestock, M., 2003. Pro-brain-derived neurotrophic factor is decreased in parietal cortex in Alzheimer's disease. Brain Res. Mol. Brain Res. 111, 148–154.

Michalski, B., et al., 2015. Brain-derived neurotrophic factor and TrkB expression in the "oldest-old," the 90 + study: correlation with cognitive status and levels of soluble amyloid-beta. Neurobiol. Aging 36, 3130–3139.

Miranda, E., Lomas, D.A., 2006. Neuroserpin: a serpin to think about. Cell. Mol. Life Sci. 63, 709–722.

Mizoguchi, H., et al., 2011. Matrix metalloproteinase-9 contributes to kindled seizure development in pentylenetetrazole-treated mice by converting pro-BDNF to mature BDNF in the hippocampus. J. Neurosci. 31, 12963–12971.

Mowla, S.J., et al., 1999. Differential sorting of nerve growth factor and brain-derived neurotrophic factor in hippocampal neurons. J. Neurosci. 19, 2069–2080.

Mufson, E.J., et al., 1989. Loss of nerve growth factor receptor-containing neurons in Alzheimer's disease: a quantitative analysis across subregions of the basal forebrain. Exp. Neurol. 105, 221–232.

Mufson, E.J., et al., 2000. Loss of nucleus basalis neurons containing trkA immunoreactivity in individuals with mild cognitive impairment and early Alzheimer's disease. J. Comp. Neurol. 427, 19–30.

Mufson, E.J., et al., 2007. Cholinotrophic molecular substrates of mild cognitive impairment in the elderly. Curr. Alzheimer Res. 4, 340–350.

Mufson, E.J., et al., 2012. Hippocampal proNGF signaling pathways and beta-amyloid levels in mild cognitive impairment and Alzheimer disease. J. Neuropathol. Exp. Neurol. 71, 1018–1029.

Nonomura, T., Hatanaka, H., 1992. Neurotrophic effect of brain-derived neurotrophic factor on basal forebrain cholinergic neurons in culture from postnatal rats. Neurosci. Res. 14, 226–233.

Oddo, S., et al., 2003. Triple-transgenic model of Alzheimer's disease with plaques and tangles: intracellular Abeta and synaptic dysfunction. Neuron 39, 409–421.

Pagenstecher, A., et al., 1998. Differential expression of matrix metalloproteinase and tissue inhibitor of matrix metalloproteinase genes in the mouse central nervous system in normal and inflammatory states. Am. J. Pathol. 152, 729–741.

Pang, P.T., et al., 2004. Cleavage of proBDNF by tPA/plasmin is essential for long-term hippocampal plasticity. Science 306, 487–491.

Parachikova, A., et al., 2007. Inflammatory changes parallel the early stages of Alzheimer disease. Neurobiol. Aging 28, 1821–1833.

Parra-Damas, A., et al., 2014. Crtc1 activates a transcriptional program deregulated at early Alzheimer's disease-related stages. J. Neurosci. 34, 5776–5787.

Parra-Damas, A., et al., 2017 Jan 15. CRTC1 function during memory encoding is disrupted in neurodegeneration. Biol. Psychiatry 81 (2), 111–123. http://dx.doi.org/10.1016/j.biopsych.2016.06.025. Epub 2016 Jul 11.

Pearson, R.C., et al., 1983. Persistence of cholinergic neurons in the basal nucleus in a brain with senile dementia of the Alzheimer's type demonstrated by immunohistochemical staining for choline acetyltransferase. Brain Res. 289, 375–379.

Pedraza, C.E., et al., 2005. Pro-NGF isolated from the human brain affected by Alzheimer's disease induces neuronal apoptosis mediated by p75NTR. Am. J. Pathol. 166, 533–543.

Peng, S., et al., 2004. Increased proNGF levels in subjects with mild cognitive impairment and mild Alzheimer disease. J. Neuropathol. Exp. Neurol. 63, 641–649.

Peng, S., et al., 2005. Precursor form of brain-derived neurotrophic factor and mature

brain-derived neurotrophic factor are decreased in the pre-clinical stages of Alzheimer's disease. J. Neurochem. 93, 1412–1421.

Peng, S., et al., 2009. Decreased brain-derived neurotrophic factor depends on amyloid aggregation state in transgenic mouse models of Alzheimer's disease. J. Neurosci. 29, 9321–9329.

Perez, S.E., et al., 2011. Cholinotrophic basal forebrain system alterations in 3xTg-AD transgenic mice. Neurobiol. Dis. 41, 338–352.

Perry, E.K., et al., 1977. Necropsy evidence of central cholinergic deficits in senile dementia. Lancet 1, 189.

Phillips, H.S., et al., 1991. BDNF mRNA is decreased in the hippocampus of individuals with Alzheimer's disease. Neuron 7, 695–702.

Pimentel, L.S., et al., 2015. The multi-target drug M30 shows pro-cognitive and anti-inflammatory effects in a rat model of Alzheimer's disease. J. Alzheimers Dis. 47, 373–383.

Qi, Y., et al., 2014. Longitudinal testing of hippocampal plasticity reveals the onset and maintenance of endogenous human Ass-induced synaptic dysfunction in individual freely behaving pre-plaque transgenic rats: rapid reversal by anti-Ass agents. Acta Neuropathol. Commun. 2, 175.

Reisine, T.D., et al., 1978. Pre- and postsynaptic neurochemical alterations in Alzheimer's disease. Brain Res. 159, 477–481.

Rosa, E., Fahnestock, M., 2015. CREB expression mediates amyloid beta-induced basal BDNF downregulation. Neurobiol. Aging 36, 2406–2413.

Rosenberg, G.A., 2009. Matrix metalloproteinases and their multiple roles in neurodegenerative diseases. Lancet Neurol. 8, 205–216.

Salehi, A., et al., 2006. Increased App expression in a mouse model of Down's syndrome disrupts NGF transport and causes cholinergic neuron degeneration. Neuron 51, 29–42.

Sarter, M., et al., 2003. Attentional functions of cortical cholinergic inputs: what does it mean for learning and memory? Neurobiol. Learn. Mem. 80, 245–256.

Schmitz, T.W., et al., 2016. Basal forebrain degeneration precedes and predicts the cortical spread of Alzheimer's pathology. Nat. Commun. 7, 13249.

Schulte-Herbruggen, O., et al., 2008. Age-dependent time course of cerebral brain-derived neurotrophic factor, nerve growth factor, and neurotrophin-3 in APP23 transgenic mice. J. Neurosci. Res. 86, 2774–2783.

Scott, S.A., et al., 1995. Nerve growth factor in Alzheimer's disease: increased levels throughout the brain coupled with declines in nucleus basalis. J. Neurosci. 15, 6213–6221.

Seidah, N.G., et al., 1996. Cellular processing of the nerve growth factor precursor by the mammalian pro-protein convertases. Biochem. J. 314 (Pt 3), 951–960.

Selkoe, D.J., 2002. Alzheimer's disease is a synaptic failure. Science 298, 789–791.

Semenenko, F.M., et al., 1985. Development of a mouse antiperoxidase secreting hybridoma for use in the production of a mouse PAP complex for immunocytochemistry and as a parent cell line in the development of hybrid hybridomas. Histochemistry 83, 405–408.

Shankar, G.M., et al., 2008. Amyloid-beta protein dimers isolated directly from Alzheimer's brains impair synaptic plasticity and memory. Nat. Med. 14, 837–842.

Sims, N.R., et al., 1983. Presynaptic cholinergic dysfunction in patients with dementia. J. Neurochem. 40, 503–509.

Taylor, S., et al., 2010. A practical approach to RT-qPCR-publishing data that conform to the MIQE guidelines. Methods 50, S1–5.

Terry, R.D., 1997. The pathology of Alzheimer's disease: numbers count. Ann. Neurol. 41, 7.

Thoenen, H., 1995. Neurotrophins and neuronal plasticity. Science 270, 593–598.

Venero, J.L., et al., 1994. Expression of neurotrophin and trk receptor genes in adult rats with fimbria transections: effect of intraventricular nerve growth factor and brain-derived neurotrophic factor administration. Neuroscience 59, 797–815.

Vogels, O.J., et al., 1990. Cell loss and shrinkage in the nucleus basalis Meynert complex in Alzheimer's disease. Neurobiol. Aging 11, 3–13.

Walsh, D.M., et al., 2002. Naturally secreted oligomers of amyloid beta protein potently inhibit hippocampal long-term potentiation in vivo. Nature 416, 535–539.

Whitehouse, P.J., et al., 1982. Alzheimer's disease and senile dementia: loss of neurons in the basal forebrain. Science 215, 1237–1239.

Willand, M.P., et al., 2016. Electrical muscle stimulation elevates intramuscular BDNF and GDNF mRNA following peripheral nerve injury and repair in rats. Neuroscience 334, 93–104.

Wilson, E.N., et al., 2016. Intraneuronal Amyloid Beta Accumulation Disrupts Hippocampal CRTC1-Dependent Gene Expression and Cognitive Function in a Rat Model of Alzheimer Disease. In: Cereb Cortex.

Wilson, E.N., et al., 2017. BACE1 inhibition by microdose lithium formulation NP03 rescues memory loss and early stage amyloid neuropathology. Transl. Psychiatry 7, e1190.

Wong, T.P., et al., 1999. Reorganization of cholinergic terminals in the cerebral cortex and hippocampus in transgenic mice carrying mutated presenilin-1 and amyloid precursor protein transgenes. J. Neurosci. 19, 2706–2716.

Yang, J., et al., 2014. proBDNF negatively regulates neuronal remodeling, synaptic transmission, and synaptic plasticity in hippocampus. Cell Rep. 7, 796–806.

Zack, G.W., Rogers, W.E., Latt, S.A., 1977. Automatic measurement of sister chromatid exchange frequency. J. Histochem. Cytochem. 25 (7), 741–753.